AD NUMBER

AD875233

LIMITATION CHANGES

TO:

Approved for public release; distribution is unlimited.

FROM:

Distribution authorized to U.S. Gov't. agencies and their contractors; Critical Technology; JUL 1970. Other requests shall be referred to U.S. Army Aviation Materiel Laboratories, Fort Eustis, VA 23604. This document contains export-controlled technical data.

AUTHORITY

USAAMRDL ltr, 23 Jun 1971

AD

USAAVLABS TECHNICAL REPORT 70-32C

2400°F UNCOOLED TURBINE/MATERIAL PROGRAM

VOLUME III

FLUIDIC TEMPERATURE-SENSING SYSTEM EVALUATION

By

R. P. Craig

F. Weber

July 1970

U. S. ARMY AVIATION MATERIEL LABORATORIES
FORT EUSTIS, VIRGINIA

CONTRACT DA 44-177-AMC-183(T)

AiRESEARCH MANUFACTURING COMPANY
A DIVISION OF THE GARRETT CORPORATION
PHOENIX, ARIZONA

DISCLAIMERS

The findings in this report are not to be construed as an official Department of the Army position unless so designated by other authorized documents.

When Government drawings, specifications, or other data are used for any purpose other than in connection with a definitely related Government procurement operation, the United States Government thereby incurs no responsibility nor any obligation whatsoever; and the fact that the Government may have formulated, furnished, or in any way supplied the said drawings, specifications, or other data is not to be regarded by implication or otherwise as in any manner licensing the holder or any other person or corporation, or conveying any rights or permission, to manufacture, use, or sell any patented invention that may in any way be related thereto.

DISPOSITION INSTRUCTIONS

Destroy this report when no longer needed. Do not return it to the originator.

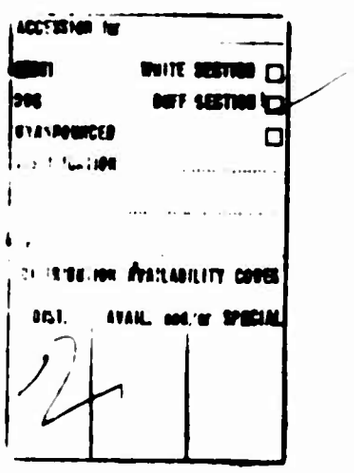

DEPARTMENT OF THE ARMY
HEADQUARTERS US ARMY AVIATION MATERIEL LABORATORIES
FORT EUSTIS, VIRGINIA 23604

The research described herein was conducted by the AiResearch Manufacturing Company, Phoenix, Arizona, under U. S. Army Contract DA 44-177-AMC-183(T). The work was performed under the technical management of Lawrence E. Bell, Jr., Propulsion Division, U. S. Army Aviation Materiel Laboratories.

Appropriate technical personnel of this Command have reviewed this report and concur with the conclusions and recommendations contained herein.

This document is Volume III of a three-volume report and covers the evaluation of a fluidic temperature-sensor system. Volume I covers the high-temperature materials investigations conducted under the above-mentioned contract, and Volume II covers the high-temperature turbine design.

Task 1G162203D14413
Contract DA 44-177-AMC-183(T)
USAAVLABS Technical Report 70-32C
July 1970

2400°F UNCOOLED TURBINE/MATERIAL PROGRAM

VOLUME III

FLUIDIC TEMPERATURE-SENSING SYSTEM EVALUATION

By

R. P. Craig
F. Weber

Prepared by

AiResearch Manufacturing Company
A Division of The Garrett Corporation
Phoenix, Arizona

for

U. S. ARMY AVIATION MATERIEL LABORATORIES
FORT EUSTIS, VIRGINIA

ABSTRACT

In May 1964, a USAAVLABS-sponsored turbine/material research program was initiated by the AiResearch Manufacturing Company of Arizona. The overall program objective was to advance 1964 turbine component technology to a level that would facilitate the development of an uncooled turbine capable of operation at a turbine inlet temperature of 2400°F and a pressure ratio of 10:1. The turbine was to have application in a small gas turbine engine in the 5.0-pound-per-second airflow class. The design of the uncooled turbine was based on the feasibility of developing an intermetallic beryllide material with properties sufficient for the turbine components. Benefits to be derived from such a turbine include significant improvements in power-to-weight ratio and specific fuel consumption (SFC) over that demonstrated by 1964 gas turbine engines of comparable size.

As reported in Volume I (Materials Investigation) of the uncooled-turbine program final report, a 2400°F cascade test rig that could simulate temperature conditions encountered during starting and normal operation of a 2400°F turbine was designed and developed. In view of the availability of this high-temperature test equipment, the USAAVLABS contract was modified in June 1965 to include the design and experimental evaluation of a fluidic temperature sensor for application in the uncooled turbine. This volume (Volume III of three volumes) of the uncooled-turbine program final report describes the fluidic temperature-sensor program that was conducted.

The fluidic temperature-sensor program was conducted as a joint effort between AiResearch and the Honeywell Systems and Research Division. The design and fabrication of the sensor cavity and the location and selection of the output transducer were the responsibility of Honeywell. AiResearch designed the rig mounting system for the sensor, sensor pickup probe, and sensor rig mount; provided all test instrumentation and equipment; and accomplished all of the evaluation testing.

The program included:

1. The procurement and analytical evaluation of a fluidic temperature-sensing system design.

2. Selection of materials for a breadboard-type fluidic temperature sensor to fit the preliminary requirements of the 2400°F cascade test rig.

3. Checkout and calibration of the sensor and instrumentation mounted on the breadboard bench test rig.

4. Experimental investigation of the sensor performance under varying conditions in the 2400°F cascade test rig.

5. Analyses of the experimental investigation and recommendations for future activities.

Based on the results of the test-evaluation program, it was concluded that without additional research and development efforts it was not feasible to utilize the tested fluidic temperature sensor in a 2400°F turbine.

BLANK PAGE

FOREWORD

In May 1964, a 2400°F uncooled-turbine program was initiated in compliance with Contract DA 44-177-AMC-183(T), Task 1G162203D14413. The program was conducted under the control of the United States Army Aviation Materiel Laboratories (USAAVLABS), Fort Eustis, Virginia, by the AiResearch Manufacturing Company of Arizona, a division of The Garrett Corporation.

The analytical, experimental, and developmental efforts that were conducted to conclude the subject program are described in the three volumes of the final report.

Volume I presents the results of material investigations (both USAAVLABS- and company-sponsored) that were conducted to develop a material that would be suitable for the turbine components of a 2400°F uncooled turbine.

Volume II presents the results of the aerodynamic, thermodynamic, and mechanical design activities that were conducted for the design of a 2400°F uncooled turbine.

Volume III, which is this document, presents the results of a test-evaluation program that was conducted to determine the feasibility of a fluidic temperature-sensing system for the measurement of turbine inlet temperatures (TIT's) in a 2400°F gas turbine engine.

The manager of the Small Gas Turbine Engine Project was Mr. D. G. Furst, and the program manager of this uncooled-turbine program was Mr. F. Weber. Principal investigators were Messrs. F. Weber, R. P. Craig, and A. E. Wilson. The overall guidance and technical direction provided by Messrs. J. White, H. Morrow, L. Bell, and D. Cale of USAAVLABS are gratefully acknowledged.

BLANK PAGE

TABLE OF CONTENTS

TABLE OF CONTENTS (Contd)

LIST OF ILLUSTRATIONS

LIST OF ILLUSTRATIONS (Contd)

LIST OF ILLUSTRATIONS (Contd)

LIST OF SYMBOLS

C	Constant peculiar to the gas and the sensor; or capacitance, farads; or a constant of integration
C_t	Thermal capacitance
d	Differential symbol for equation
e	Mathematical symbol for equation
f	Output frequency of the sensor, Hz
H(s)	Transfer function
HT	Heat transfer coefficient
K	Calibration constant
n	Calibration constant
R	Gas constant, sq ft per sec^2 per °R
r	Thermal resistance
rg	Effective thermal resistance
s	LaPlace's variable
T	Absolute temperature of the gas, °R
Tg	Effective gas temperature
To	Absolute temperature of component, °R
t	Time, sec
α	For this study, a theoretical value of 0.500
γ	Ratio of specific heats
θ	Integration with respect to time
τ	Time constant

1. INTRODUCTION

In the control of high-temperature gas turbine engines and the testing of associated components, one of the most important parameters to be measured is TIT.

The temperature-measuring device should have the following salient features:

1. Rapid response to temperature transients
2. High steady-state accuracy
3. Long life
4. Low cost

Fulfillment of the first requirement enables a more sophisticated dynamic control of the engine, such as surge protection and acceleration limiting, while the second requirement ensures that the engine operating point is well defined under all operating conditions and thereby contributes to long engine life.

However, the TIT that can be expected during normal operation in a 2400°F turbine exceeds the limit that existing temperature-sensing thermocouples can accurately sense with high response rates and yet maintain a reasonable life span. Therefore, either TIT must be inferred from thermocouples located in a less severe environment and, consequently, with less accuracy or an alternate method of TIT measurement must be developed.

The objective of this program was to investigate and determine the feasibility of using a fluidic temperature-sensing system to measure TIT's of 2400°F with transient temperatures reaching the rate of 2500°F per second. The program consisted of (a) analytical evaluations of a fluidic temperature-sensing system and (b) both bench-type and cascade-rig-type testing to determine the usefulness of the system with respect to:

1. Response to temperature transients

2. Accuracy variations

3. Reliability

4. Operation of the temperature readout systems

2. SYSTEM DESCRIPTION

2.1 GENERAL

The physical arrangement of the fluidic temperature-sensing system is shown in Figure 1. Subsequent paragraphs present a description of the pickup probe, fluidic sensor, and transducer.

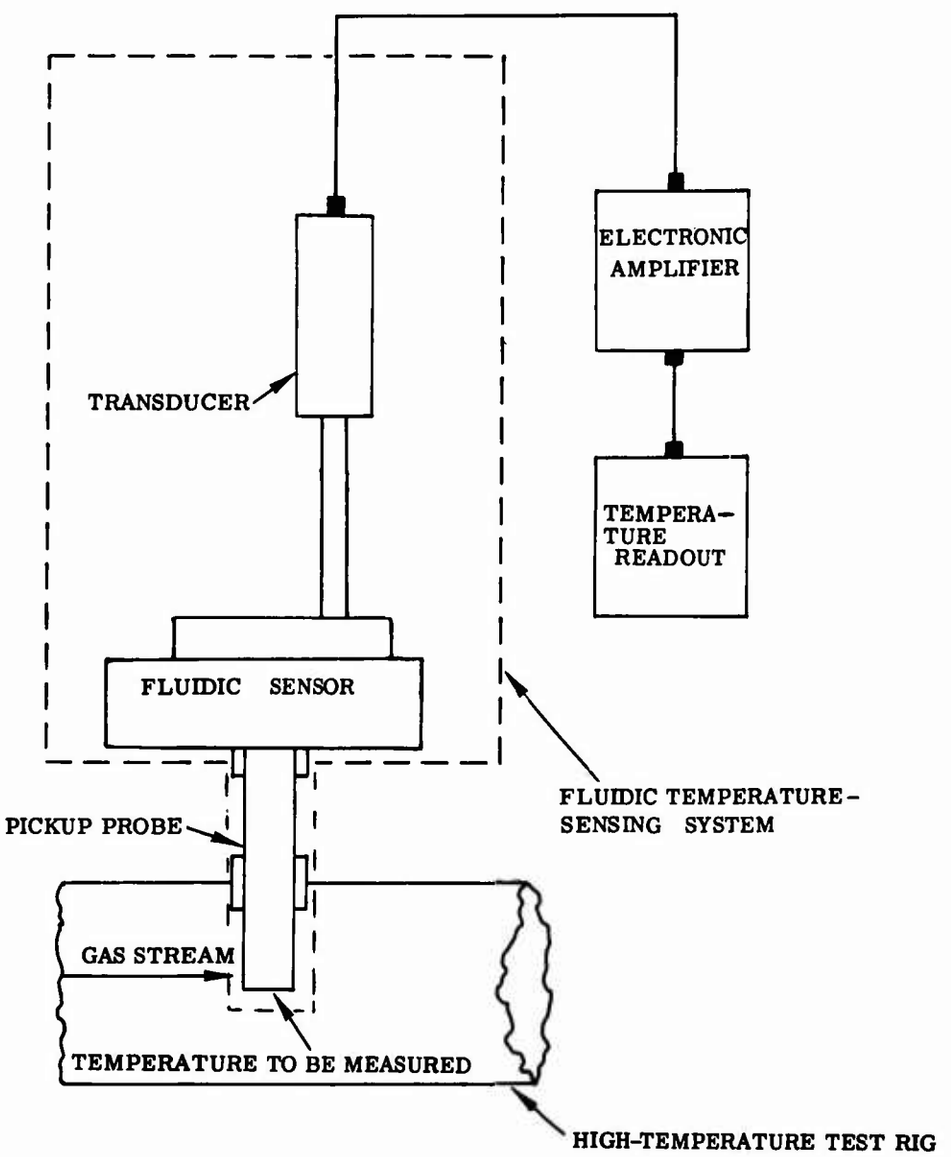

Figure 1. Fluidic Temperature-Sensing System Diagram.

2.2 PICKUP PROBE

The function of the temperature-sensing pickup probe is to sense and transmit the temperature to be measured from its source into the fluidic sensor.

The first design consideration for the probe was that of material selection. The material had to be capable of surviving steady-state temperatures of 2400°F and temperature transients reaching 2500°F per second.

Materials investigated for use in the probe included the following:

1. Alumina
2. Zirconia
3. Boron nitride
4. Fused quartz
5. Inconel 702

Preliminary material investigations revealed that both the alumina and zirconia materials were unable to withstand the transient-temperature requirement. In addition, it was determined that the boron nitride was also unsuitable because of insufficient oxidation resistance to the environmental conditions of the cascade testing.

It first appeared that the fused-quartz tubing ideally satisfied the steady-state and transient-temperature requirements. It has a melting point of approximately 1800°C (3272°F) and good thermal shock resistance due to the thermal coefficient of expansion of 0.31 in./in. °F x 10^{-6}. To test this material, specimens were ordered in two designs. The different designs as received from the vendor are shown in Figure 2. Two of the probes were lost due to a misalignment between the probe and the bench test setup, which caused a tensile force sufficient to fracture the quartz. A third probe was broken when a Hydrodyne seal was installed between the probe base and the adjacent seal. It was found that a metal O-ring provided a better seal for the probe. The fused-quartz pickup probes worked quite well, once in the test rig. However, because of the lack of low-temperature ductility, the probes were invariably damaged during installation and disassembly of the test equipment. Because they are so fragile, a quartz probe would probably not be suitable for actual engine operation.

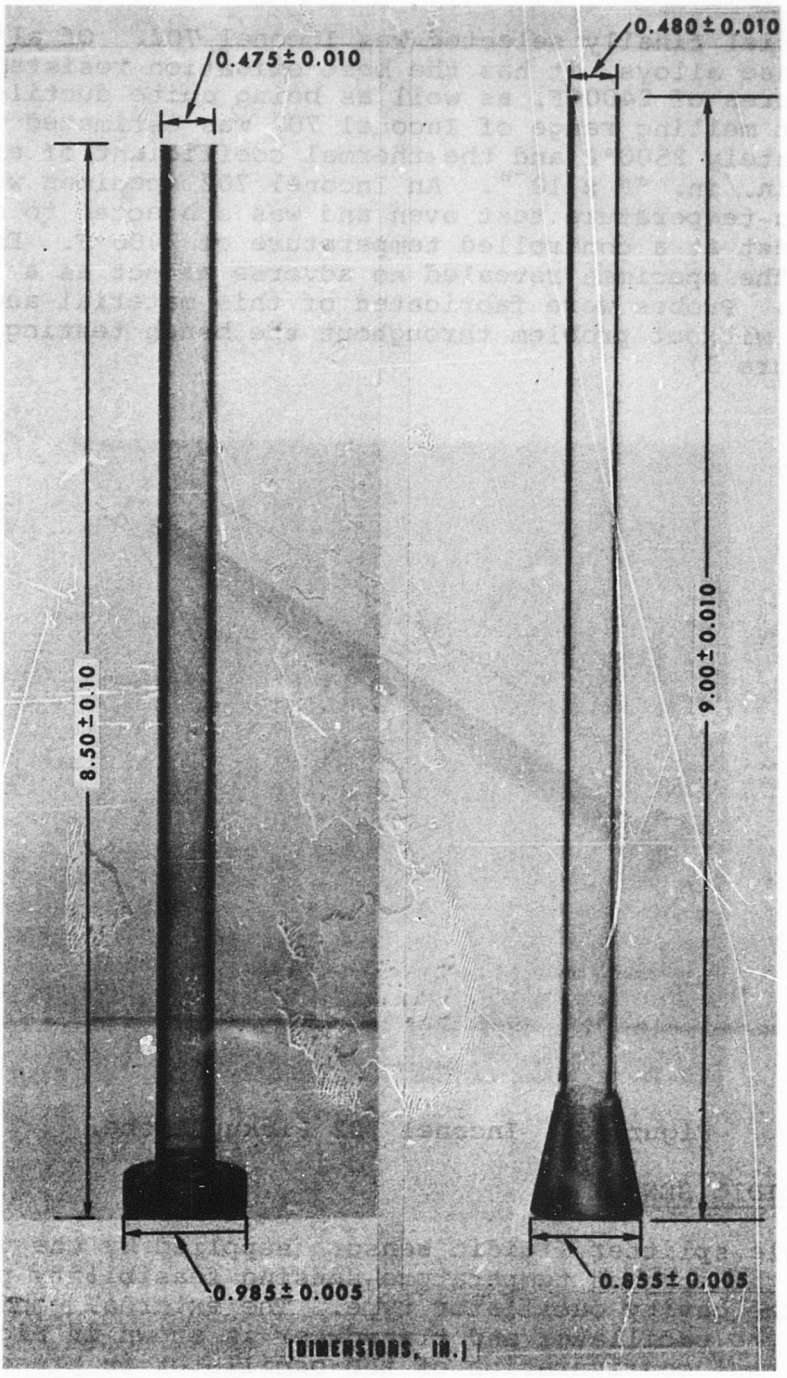

Figure 2. Two Designs of Fused-Quartz Pickup Probes.

The material finally selected was Inconel 702. Of all the nickel-base alloys, it has the best oxidation resistance at temperatures of 2400°F, as well as being quite ductile. The incipient melting range of Inconel 702 was estimated to be approximately 2500°F and the thermal coefficient of expansion is 9.25 in./in. °F x 10^{-6}. An Inconel 702 specimen was placed in a high-temperature test oven and was subjected to a 60-hour static test at a controlled temperature of 2400°F. Examination of the specimen revealed no adverse effect as a result of the test. Probes were fabricated of this material and were utilized without problem throughout the bench testing program (see Figure 3).

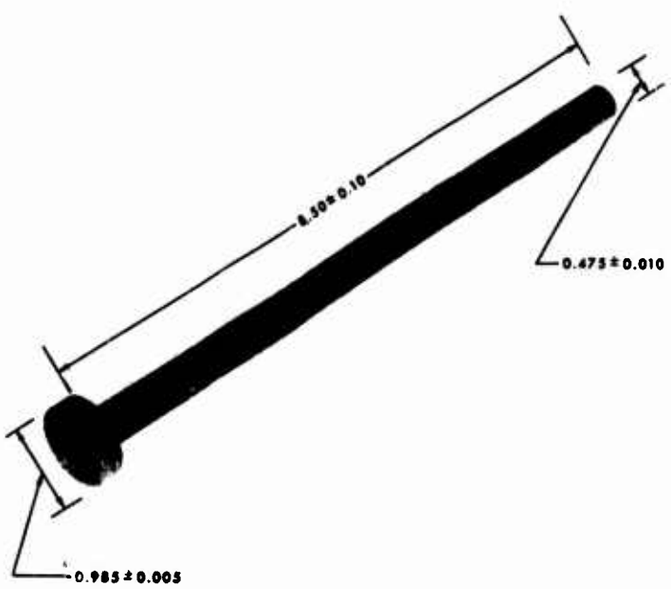

Figure 3. Inconel 702 Pickup Probe.

2.3 FLUIDIC SENSOR

The single-splitter fluidic sensor (supplied by the vendor) used in the subject temperature-sensing feasibility program was of the cavity oscillator type. The external configuration of the oscillator and transducer is shown in Figure 4. The internal configuration of the oscillator is presently classified "CONFIDENTIAL". In addition, the device contains internal features that are proprietary to the vendor. Because the oscillator was of a prototype nature, it was not

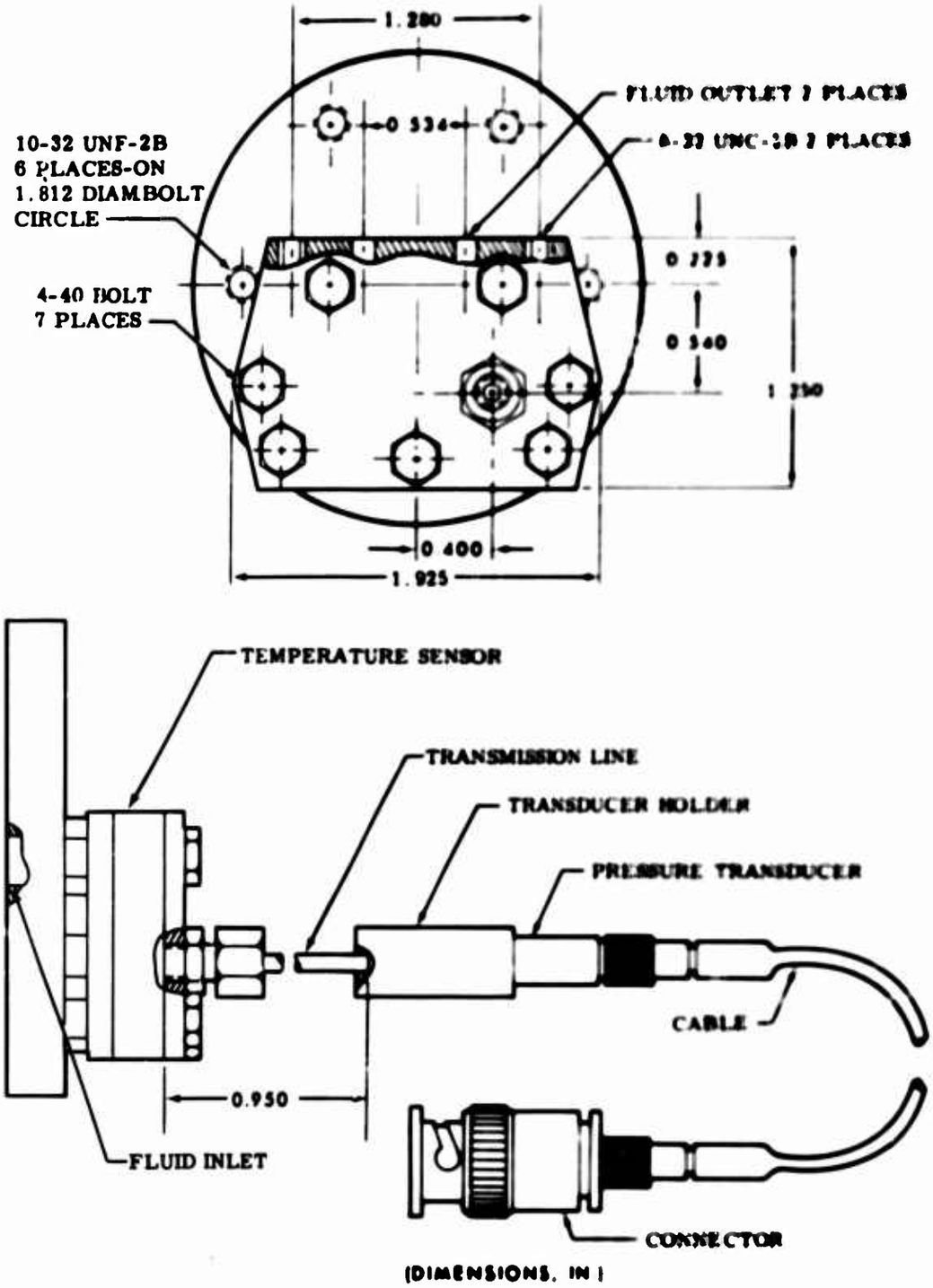

Figure 4. Fluidic Sensor External Configuration.

intended that this device provide for the ultimate user requirement but rather that it serve in the research efforts in evaluation of specific temperature-sensing problems. The material requirements, with regard to temperature, were the same as those stated for the pickup probe. However, sensor fabrication limitations led to investigation of the following materials:

1. Bendix Chrome-30.

2. Refractory metal (such as molybdenum, tantalum, or tungsten) coated with a commercially available cermet such as Rokide A, Rokide Z, or Rokide C.

3. Refractory metal with a chromium plate ion-deposited on the surface.

4. AiResist 213 (a cobalt-base alloy) with nickel aluminide inserts for the inlet and exhaust nozzles.

5. Inconel 702 (a nickel-base alloy) with high chromium (14.0 to 17.0 percent) and aluminum (2.75 to 3.25 percent) contents.

6. Inconel 702 with nickel aluminide inserts for the inlet and the exhaust nozzle regions.

Bendix Chrome-30 was eliminated due to its tendency to deteriorate rapidly at the required temperatures (as a result of a reaction with nitrogen in the air). The ability of any of the Rokide-oxide coatings to provide sufficient adherence, freedom from porosity, and thermal-shock resistance to maintain adequate coating integrity for the refractory metals was found to be inadequate for this application. Ion-deposited chromium plating on the refractory metals was eliminated for the same reasons. AiResist 213 was eliminated because incipient melting occurred at 2325°F.

The material found to be most satisfactory for this application was Inconel 702 for the same reasons presented in the pickup-probe discussion. It is a difficult material to machine, but with careful use of the proper equipment, a satisfactory part could be expected. In the final design, all metal parts, including the bolts holding the sensor plates together, were fabricated from Inconel 702.

2.4 TRANSDUCER

A standard quartz pressure transducer was used to transform the pneumatic output of the fluidic sensor into an electrical signal. The transducer had a sensitivity of approximately 1 picocoulomb per psi. The transducer output signal is directed into an electronic amplifier. The output of the electronic amplifier is directed into a general radio-frequency meter. The output of the radiofrequency meter is then filtered with an appropriate time constant.

3. SYSTEM DESIGN ANALYSES

3.1 GENERAL

The fluidic temperature sensor is a device that converts the temperature of a flowing gas into a frequency signal proportional to the square root of the absolute temperature (T) of that gas. This general definition implicitly assumes an adiabatic gas flow; i.e., no change in temperature during its flow through the sensor. As long as the sensor can be considered operating in a steady-state condition, it will function in a manner very closely described by the equation

$$f = C\sqrt{T} \tag{1}$$

where f is the output frequency of the sensor, C is a constant peculiar to the gas and the sensor, and T is the absolute temperature of the gas. This frequency signal is passed through an analog converter having a negligible time-constant to produce a direct voltage proportional to instantaneous input frequency. Thus, the direct voltage will be proportional to the square root of T_3 (t). In order to provide a voltage signal directly proportional to T_3 (t), the output signal of the frequency to the analog converter must be squared. The squared signal is then connected to the linearizing circuit. The output of the linearizing circuit will then be proportional to T_1 (t). The arrangement of the components in the complete measuring system is shown in Figure 5.

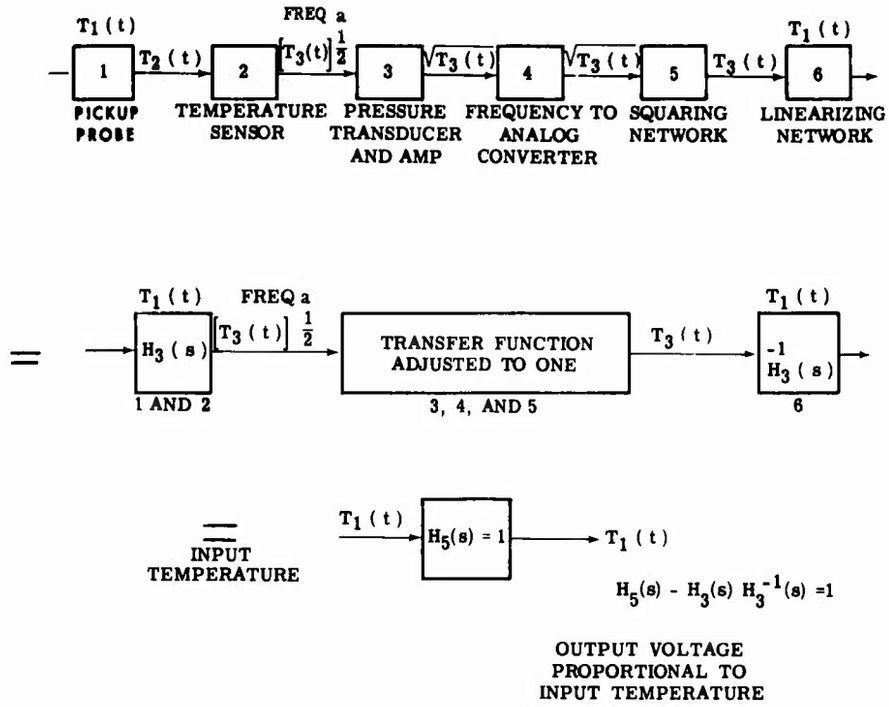

Figure 5. Arrangement of Components in the Temperature-Measuring System.

3.2 TEMPERATURE ANALYSIS

In cases where the sensor is operating in temperature conditions other than steady state, the frequency output of the senscr will indicate some value different from that of the gas temperature entering the sensor system. The difference results from the thermal "flywheel" effect of the body material. Unless the body material is the same temperature as the gas to be measured, heat transfer will occur between the body and the gas.

The determination of the transient-temperature effect on the operation of the sensor was the basic objective of this analysis. Included in this broad objective were two related areas of interest:

1. Determination of time constant of sensor probe

2. Determination of time constant of sensor body

The transient-temperature effect on the fluid-amplifier temperature sensor was determined by using a transient and steady-state two-dimensional temperature computer program. This program determined the temperature distributions as functions of time and/or the steady-state temperature distribution for systems undergoing two-dimensional heat flow. The analysis by this program was accomplished by dividing the system into a finite number of small (small being relative to the accuracy desired) elements and performing an energy balance on each element. A typical element is rectangular in planform and has four neighbors, identified by 1, 2, 3, and 4. The element may have one or more convective heat-transfer surfaces, which are wetted by a gas with effective gas temperature, T_g, and it may have heat generation, Q_1, within the point. [9] The thermal energy balance on such an element results in the equation

$$\frac{dT_o}{d\theta} = \frac{1}{C_t}\left[\frac{T_1 - T_o}{r_1} + \frac{T_2 - T_o}{r_2} + \frac{T_3 - T_o}{r_3} + \frac{T_4 - T_o}{r_4} + \frac{T_g - T_o}{r_g}\right] + Q \qquad (2)$$

With the initial temperatures, thermal resistances, and thermal capacitances of the elements given, integration with respect to time, θ, may be accomplished by numerical methods.

To use this program, the total volume was divided into small elements and the initial temperature of each element was specified. A step input for the temperature was programed. The step function and the resultant temperature response of the probe are shown in Figure 6.

The time constant of the probe is defined as the time required for the Station 3 temperature to equal 63.2 percent of the step-function temperature change, 2300°F. From Figure 6, this value is approximately 91 seconds. From Figure 6, it can also be seen that the leading point of the sensor approaches the gas temperature at a much faster rate than does the exhaust section, with a time constant equal to 12 seconds.

The value of the heat-transfer coefficient in the probe was calculated to be 7.43 Btu per (ft^2-hr-°F).

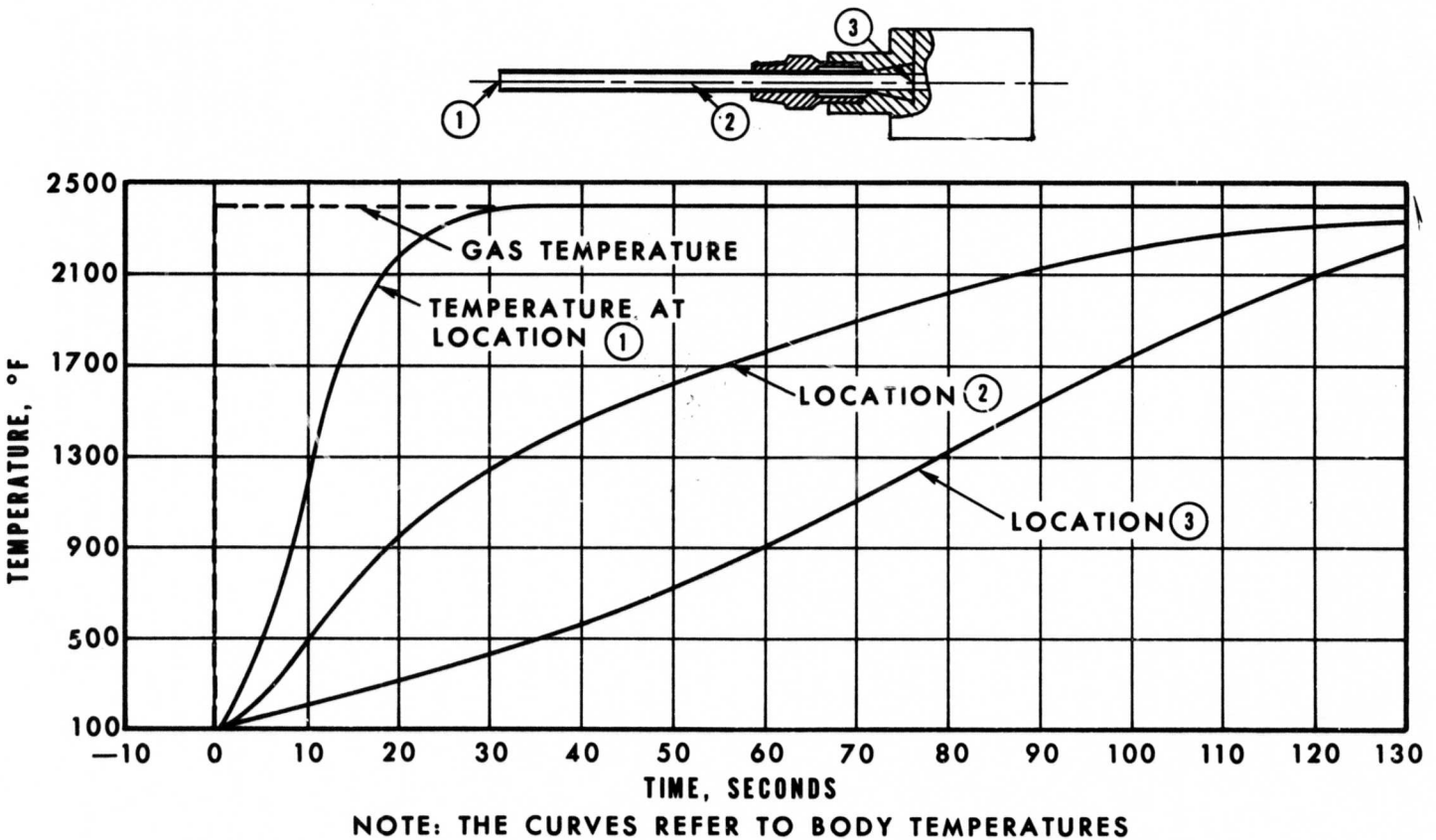

Figure 6. Results of Transient-Temperature Analysis of Pickup Probe.

Figures 7, 8, and 9 illustrate the temperature of the sensor body at critical points. Each figure is shown with three curves. The different curves demonstrate a change in the film heat-transfer coefficient. Because of the unusual shape of the body cavity and the flow patterns of the gas within the cavity, a precise determination of the heat-transfer coefficient is quite difficult. For these reasons, the film heat-transfer coefficient was analytically determined over the surface of the cavity and then varied by factors of 5 and 10 to determine the effect of the variation on the transient response of the body. The film heat-transfer coefficient was calculated to be 15.0 Btu per (ft^2-hr-°F) for Figure 7. For Figure 8, the value was determined to be 30.0 Btu per (ft^2-hr-°F); and for Figure 9, the value was found to be 8.0 Btu per (ft^2-hr-°F).

The time constant was based on Figure 9, which provides the longest time constant of the three points. From Figure 9 and the curve referring to $5HT_1$, the time constant is approximately 92 seconds. The smallest time constant of the body is from the splitters (see Figure 8), referring to curve $10HT_1$. This time constant is approximately 8.5 seconds. The rate of heating will then vary with these typical time constants--i.e., over a range from 8.5 seconds to 92 seconds--to reach 63.2 percent of the final temperature of the step function. Thus, the selected body should be capable of withstanding high-temperature transients with the resultant thermal gradients.

An estimate of the gas temperature leaving the probe (entering the sensor) was made with the use of a thermal-energy balance between the gas and the probe. In this calculation it was assumed that the probe change in temperature was due to energy absorption from the gas. Thus, by relating the change in temperature of the probe to the energy required to make that change, the resultant temperature loss of the gas was estimated. The result of this calculation is shown in Figure 10.

The time constants of both the probe and the sensor body are approximately the same: 91 and 92 seconds. These values, compared to the flushing time constant of the sensor cavity (the time required to replace a gas at one temperature completely with the gas at another temperature), are of such magnitude that the flushing time constant is undetectable. In order to actually determine the inherent response time of the sensor, these time constants must be accounted for in the electrical output system.

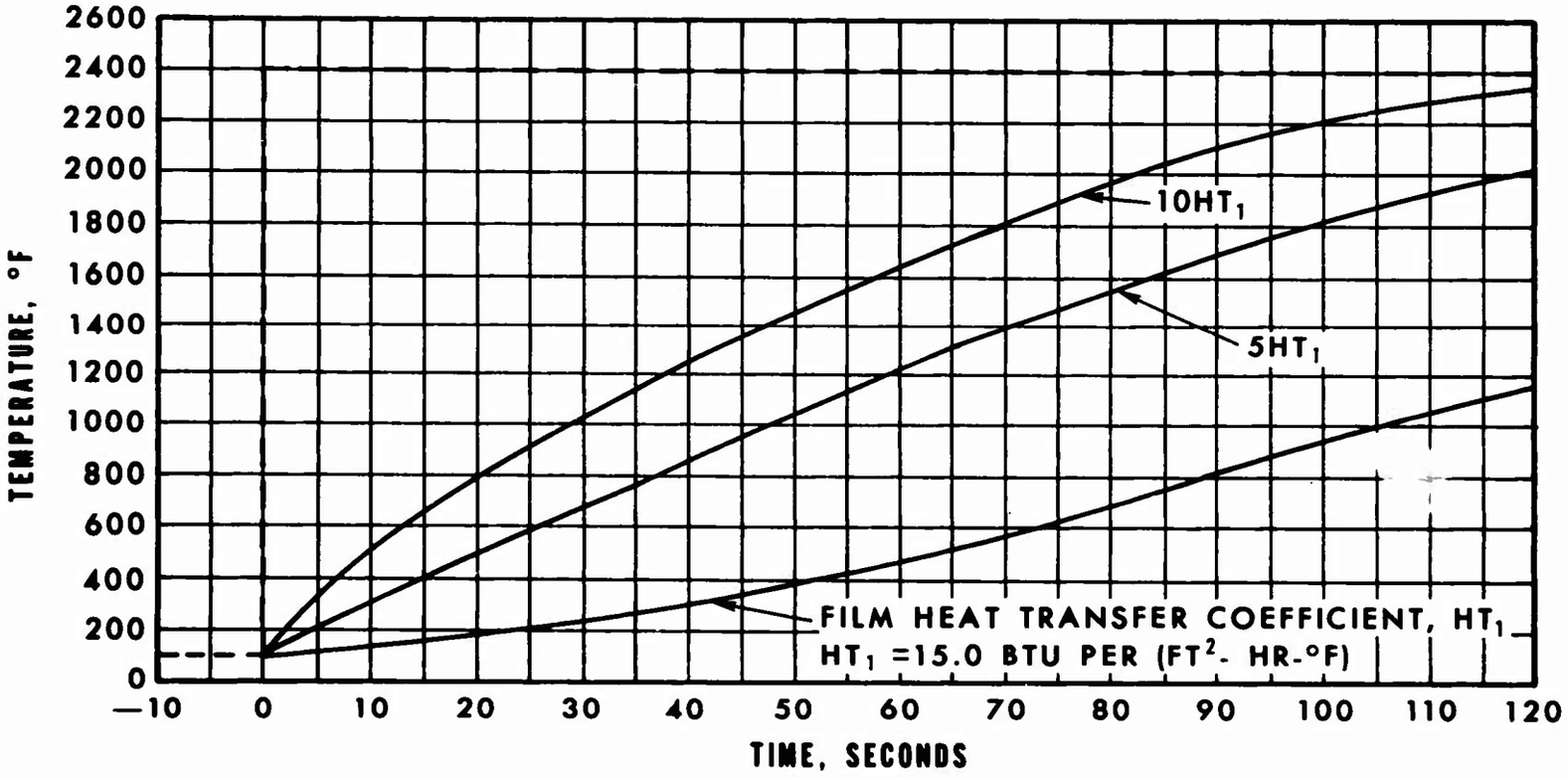

Figure 7. Results of Transient-Temperature Analysis of Sensor Body at the Inlet-Nozzle Location.

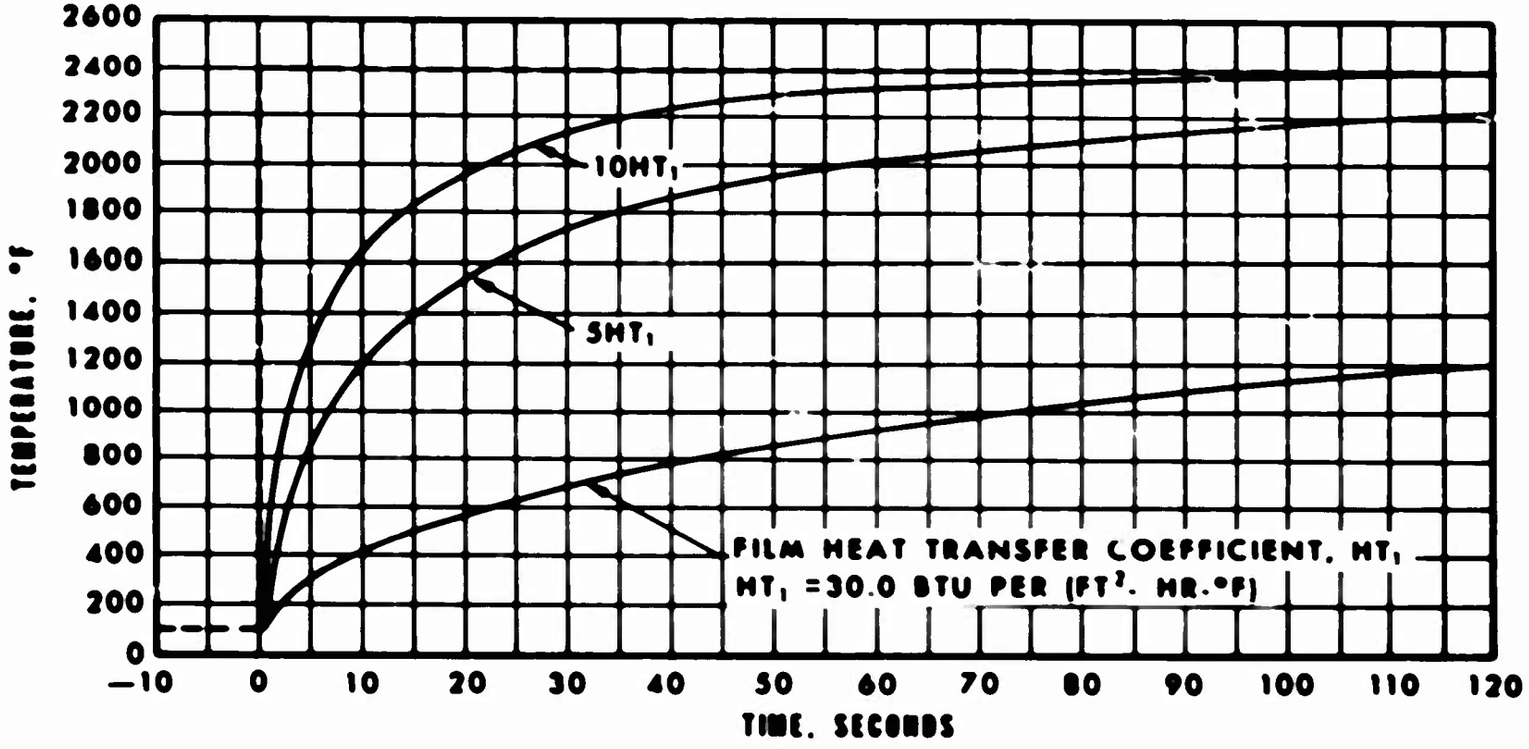

Figure 8. Results of Transient-Temperature Analysis of Sensor Body at Splitter Tip Location.

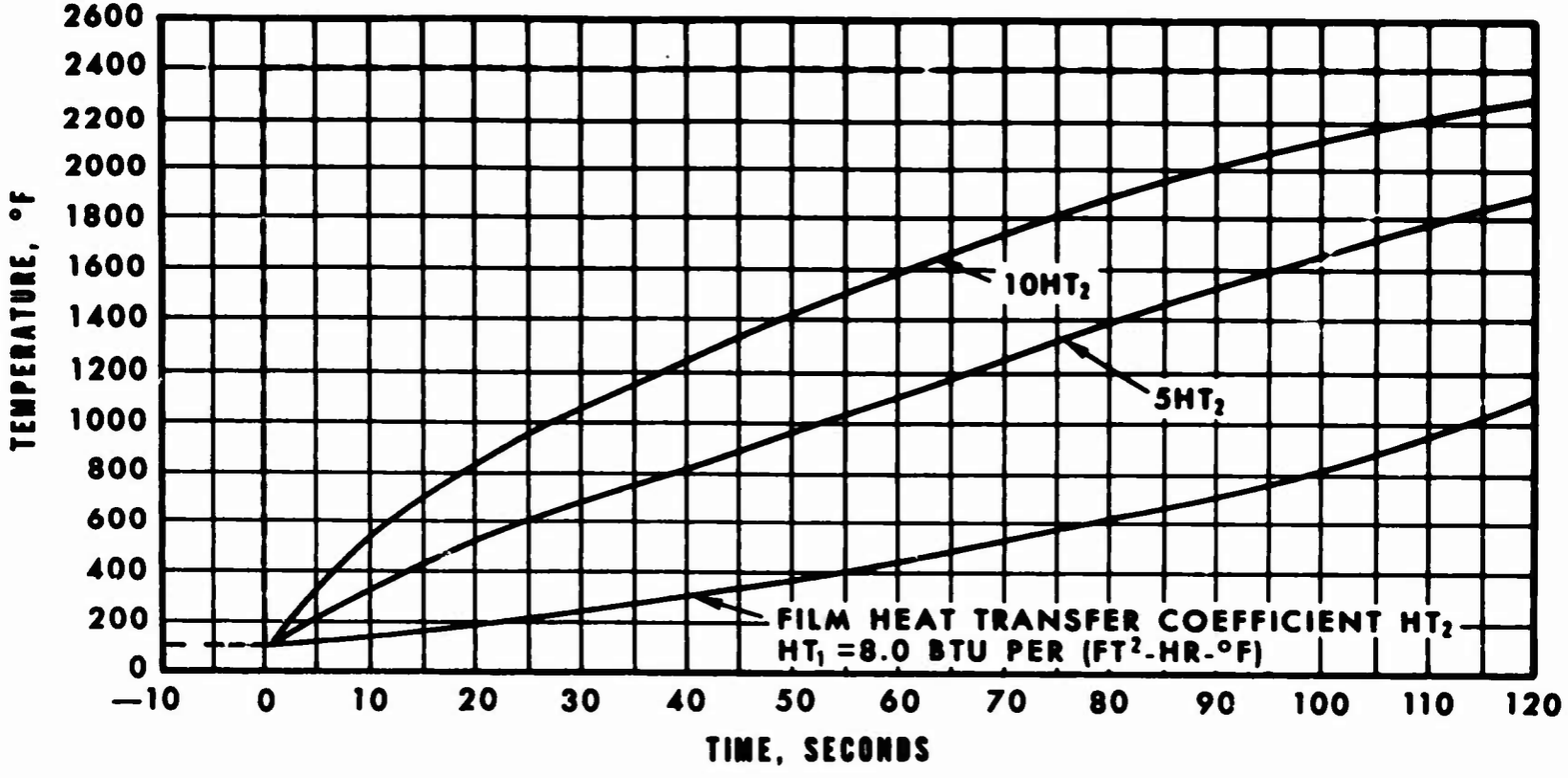

Figure 9. Results of Transient-Temperature Analysis of Sensor Body at Side-Wall Location.

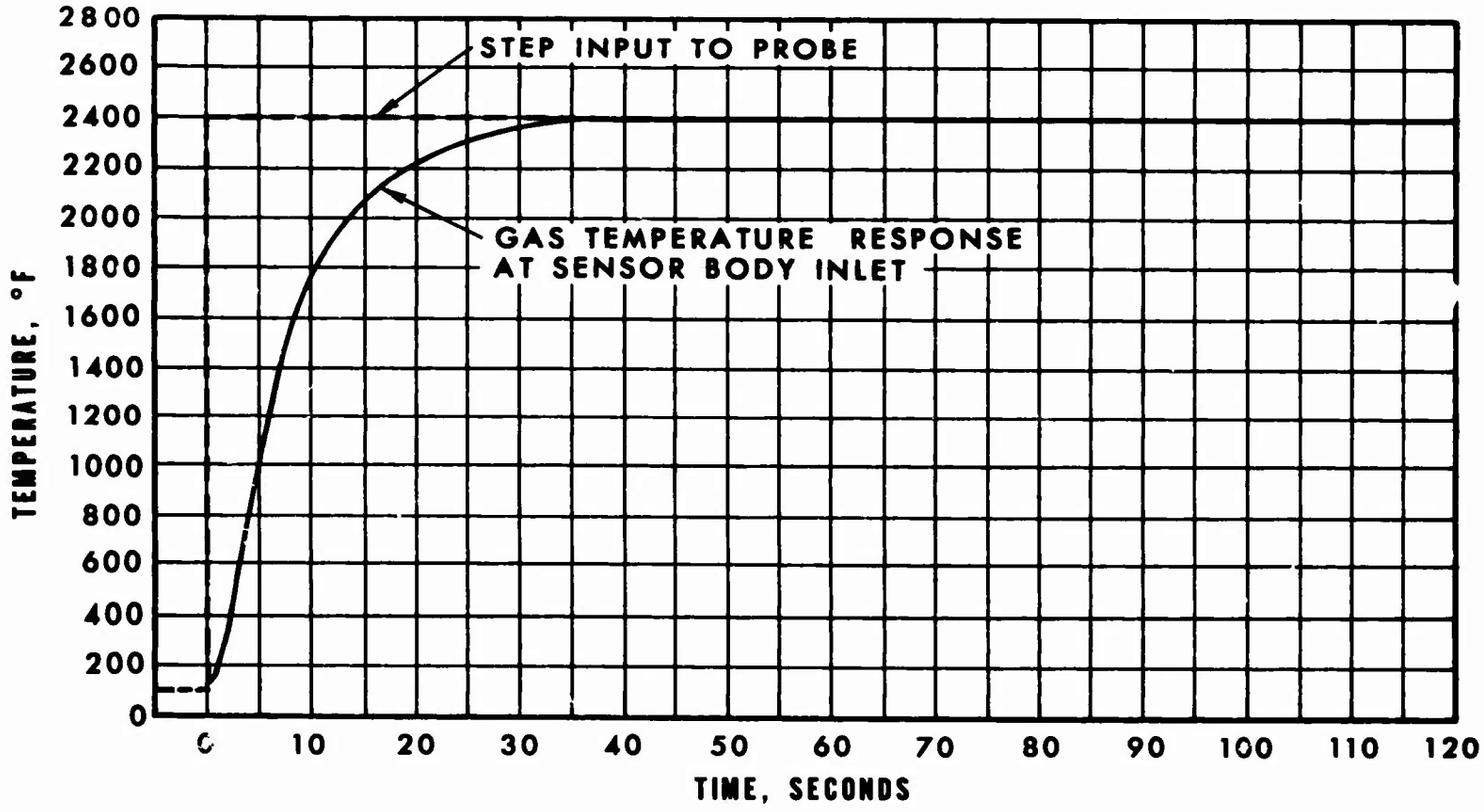

Figure 10. Sensor Body Inlet Gas Temperature Response to Probe Inlet Gas Temperature.

3.3 LINEARIZING CIRCUIT ANALYSIS

The physical arrangement of the fluidic temperature sensor is shown in Figure 11.

The linearizing network must receive a voltage signal that is proportional to $T_3(t)$. The output frequency signal is proportional to the square root of $T_3(t)$. This frequency signal is passed through a frequency to analog converter having a negligible time constant to produce a voltage directly proportional to instantaneous input frequency. Thus, the voltage will be proportional to the square root of $T_3(t)$. In order to provide a voltage signal directly proportional to $T_3(t)$, the output signal of the frequency to the analog converter must be squared. The squared signal is then connected to the linearizing circuit. The output of the linearizing circuit will then be linearly proportional to $T_1(t)$. The arrangement of the components in the complete measuring system is shown in Figure 5 (page 11).

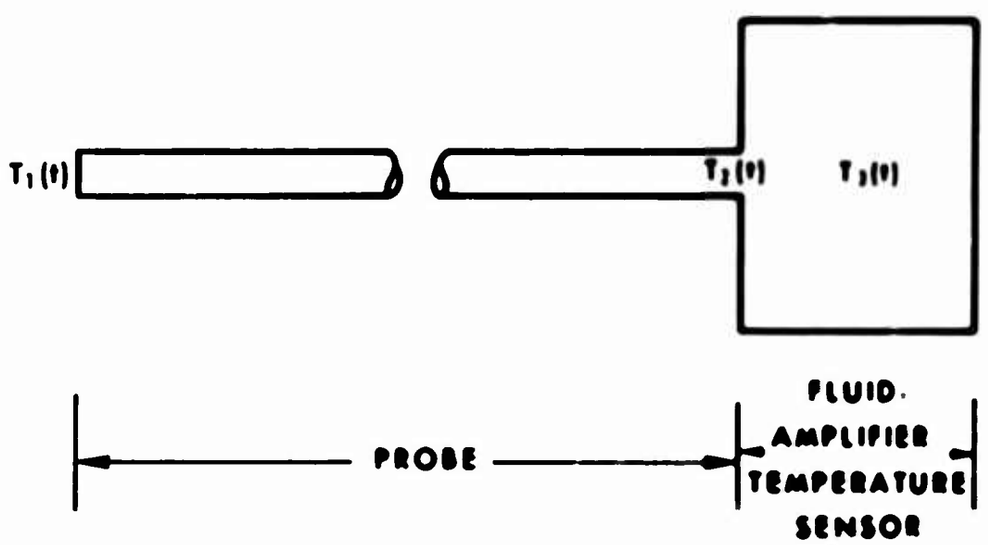

$T_1(t)$ - TEMPERATURE TO BE MEASURED

$T_2(t)$ - PROBE OUTPUT TEMPERATURE WHICH IS THE SENSOR INPUT TEMPERATURE

$T_3(t)$ - TEMPERATURE ACTUALLY SENSED

Figure 11. Physical Arrangement of Probe and Temperature Sensor.

The input temperature to the sensor is related to the output frequency by Equation 3:

$$T = \frac{\frac{1}{f^{\alpha}}}{K\gamma R} \tag{3}$$

where

T = absolute temperature of the gas, °R

f = output frequency, Hz

K = a constant

γ = ratio of specific heats (dimensionless)

R = gas constant, sq ft per sec^2 per °R

Thus, the output frequency is related to the input temperature by the Mach number relationship to the gas, such as

$$f = [K\gamma R]^{\alpha} T^{\alpha} \tag{4}$$

This theoretical consideration fixes the value of α at 0.500; however, in practice, this value is somewhat lower. The frequency signal is converted to a voltage level signal through the use of a frequency discriminator. The output of the frequency discriminator is fed to the linearizer circuit. A block outline of the system is shown in Figure 12.

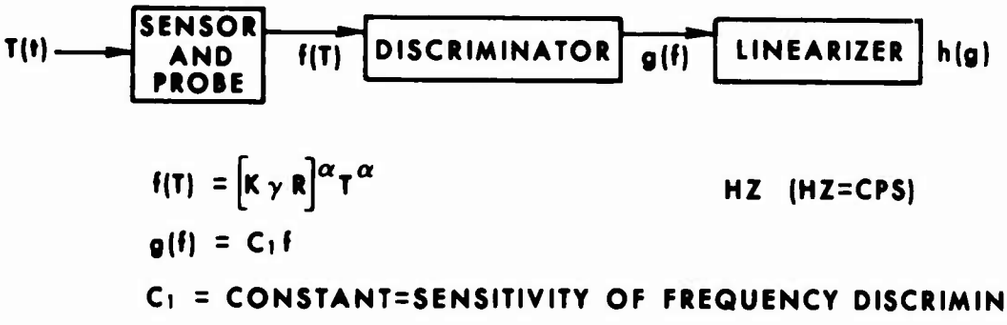

Figure 12. Block Outline of Temperature-Measuring System.

Since f, g, and h are all increasing functions of their respective single variables, each function takes on its maximum value at the maximum value of its variable. That is,

$$f_{MAX} = f\ (T_{MAX}) \qquad g_{MAX} = g(f_{MAX}) \qquad h_{MAX} = h(g_{MAX})$$

We have

$$g(T) = C_1 [K\gamma R]^{\alpha} T^{\alpha} \tag{5}$$

and

$$\frac{dg(T)}{dT} = \alpha C_1 [K\gamma R]^{\alpha} T^{\alpha-1} \tag{6}$$

We desire h(g) to be a linear function of T. Thus,

$$h(g) = h(C_1 [K\gamma R]^{\alpha} T^{\alpha}) = C_2 T \tag{7}$$

Where C_2 is a constant, differentiate both sides with respect to T_1 giving

$$\frac{dh(g)}{dT} = \frac{dh}{dg}\frac{dg}{dT} = C_2 \tag{8}$$

or

$$\frac{dh(g)}{dT} = \alpha C_1 [K\gamma R]^{\alpha} T^{\alpha-1} \frac{dh}{dg} \tag{9}$$

since

$$\frac{dg(T)}{dT} = \alpha C_1 [K\gamma R]^{\alpha} T^{\alpha-1} \tag{10}$$

But

$$\frac{dh}{dg} = \frac{C_2}{\alpha C_1 [K\gamma T]^{\alpha} T^{\alpha-1}} \tag{11}$$

Giving

$$\frac{dh}{dg} = \frac{C_2 T}{\alpha g} \tag{12}$$

and since

$$h(g) = C_2 T \tag{13}$$

then

$$\frac{dh}{dg} = \frac{h}{\alpha g} \tag{14}$$

So

$$\frac{dh}{h} = \frac{1}{\alpha}\frac{dg}{g} \tag{15}$$

Integrating gives

$$\ln h = \frac{1}{\alpha} \ln g + \ln C_3 \tag{16}$$

where C_3 is a constant of integration

We have then, from Equation (16),

$$h = C_3 \, g^{1/\alpha} \tag{17}$$

Therefore,

$$C_2 = \frac{C_3 g^{1/\alpha}}{T} = C_3 C_1^{1/\alpha} [K\gamma R] \tag{18}$$

Thus,

$$h = C_3 C_1^{1/\alpha} [K\gamma R] T = C_3 g^{1/\alpha} \tag{19}$$

3.4 AMPLITUDE SCALING

Letting T take on its maximum expected value, designated as T_o, gives

$$f_{max} = [K\gamma R]^{\alpha} T_o^{\alpha} \tag{20}$$

Then

$$g_{max} = C_1 f_{max} \tag{21}$$

Setting the maximum value of the analog variable, g_{max}, as 10 volts gives

$$C_1 = \frac{10}{f_{max}} = \frac{10}{[K\gamma R]^{\alpha} T_o^{\alpha}} \tag{22}$$

Then

$$C_2 = C_3 C_1^{1/\alpha} [K\gamma R] = \frac{10^{1/\alpha}}{T_o} C_3 \tag{23}$$

The maximum value of the analog variable h(g), is set by g_{max}; thus,

$$h_{max} = C_3 (g_{max})^{1/\alpha} = C_3 10^{1/\alpha} \text{ volts} \tag{24}$$

Setting

$h_{max} = 10$ volts, gives for C_3:

$$C_3 = \frac{10}{10^{1/\alpha}} = 10^{-\frac{(1-\alpha)}{\alpha}} \tag{25}$$

Then

$$h = C_3 g^{1/\alpha} = 10^{-\frac{(1-\alpha)}{\alpha}} g^{1/\alpha} \tag{26}$$

Note that the form of h(g) is dependent only on α.

From Equations (7), (23), and (25):

$$h(g) = C_2 T = \frac{10^{1/\alpha}}{T_o} C_3 T$$

$$= 10^{1/\alpha} 10^{-\frac{(1-\alpha)}{\alpha}} \frac{T}{T_o} \tag{27}$$

Therefore,

$$h(T) = 10^{\frac{T}{T_o}} \tag{28}$$

A variable diode function generator (VDFG) was used to generate Equation (26). The input voltage was g(f), and the output voltage was h(g). A VDFG is an active network utilizing operational amplifiers, resistors, and semiconductor diodes.

3.5 VENDOR PERFORMANCE TESTS

Performance testing of the fluidic sensor was accomplished by the vendor prior to delivery of the sensor and the bench testing reported in Section 4. The following subparagraphs present a summary of the vendor's findings:

3.5.1 Operating Characteristics

A steady-state calibration curve for the fluidic sensor operating on air is shown in Figure 13. This figure also contains the steady-state calibration constants K and n for the analytical expression $T = \frac{f^n}{K\gamma R}$. Another operating characteristic of importance is the frequency sensitivity as a function of inlet pressure. This is given in Figure 14.

Dimensional changes in the fluidic sensor due to heating will affect the output frequency. This change is taken into account in the calibration curve (Figure 13) for the fluidic sensor operating in ambient air.

The flow rate of the fluidic sensor is given in Figure 14 in standard cubic feet per minute for air.

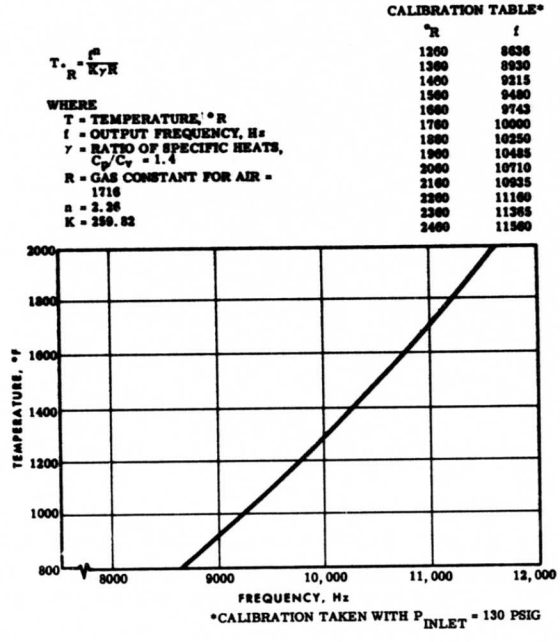

Figure 13. Calibration Curve for Fluidic Temperature Sensor.

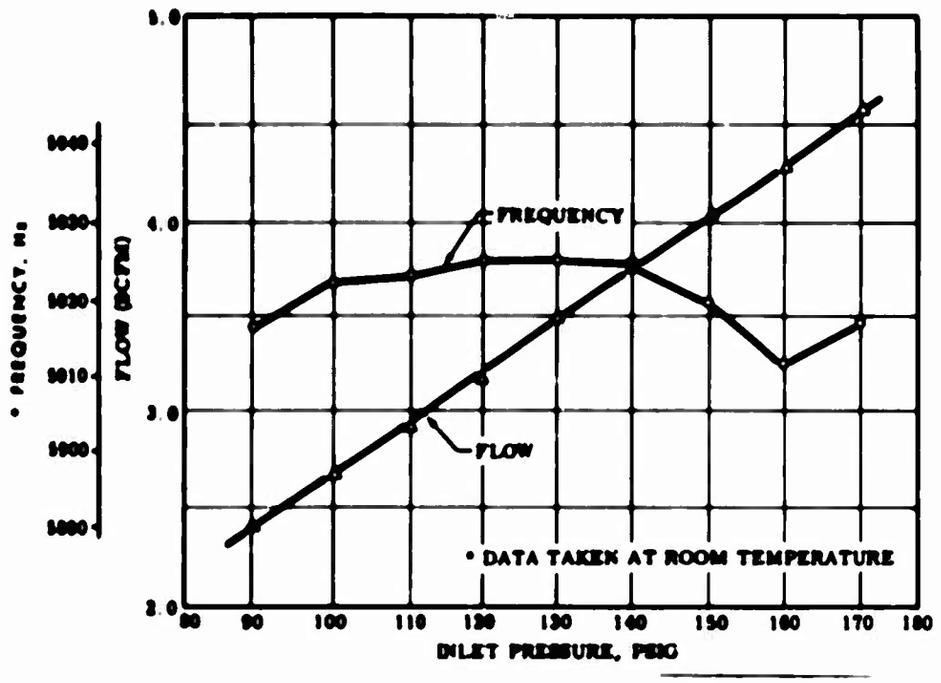

Figure 14. Performance Curves for Fluidic Temperature Sensor.

3.5.2 Dynamic Response

The fluidic sensor exhibits a double time constant in its dynamic response. The following form is to be expected of the sensor:

$$T = \frac{f^n}{K_V R} \left[\frac{K_1}{T_1 s + 1} + \frac{K_2}{T_2 s + 1} \right] \qquad (29)$$

Figure 15 is a curve showing time response and gives the constant mentioned above. It should be noted that the use of an electronic lead network of the form $K_2 \left(\frac{Ts}{Ts+1}\right)$ will do much to take care of the second time constant and so enhance the overall response of the fluidic sensor. Figure 16 is a schematic diagram of such a compensating lead network.

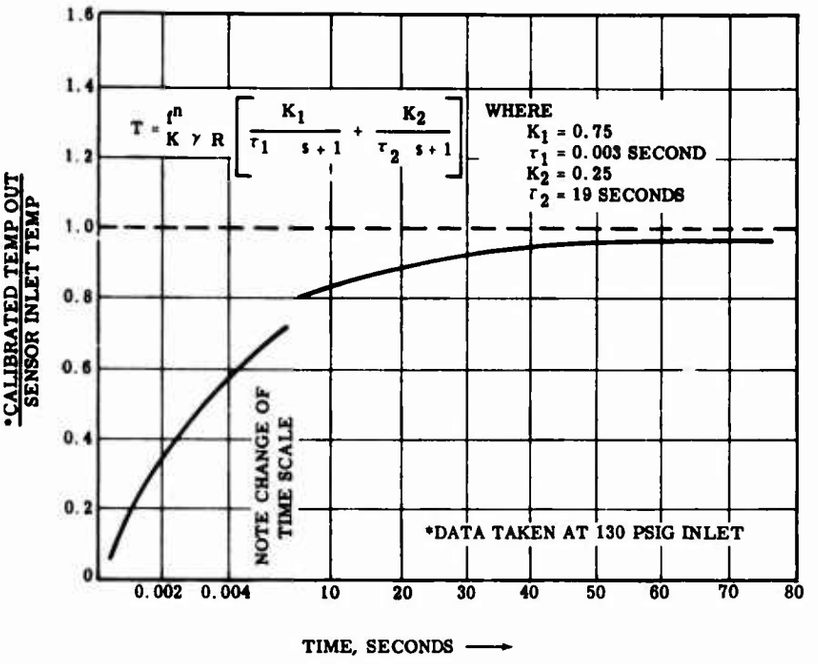

Figure 15. Step Response for Fluidic Temperature Sensor.

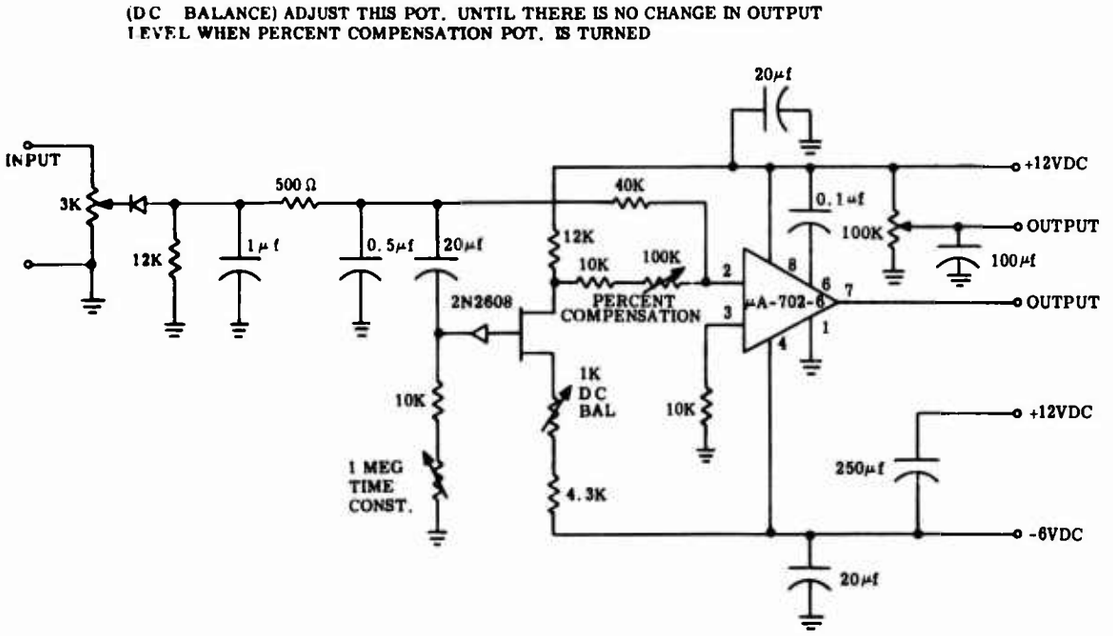

Figure 16. Compensating Lead Network.

4. SYSTEM BENCH TESTS

4.1 GENERAL

Upon receipt of the fluidic sensor from the vendor, a bench-test rig was constructed with which preliminary evaluations were conducted on the temperature-sensing system. The bench-test rig provided for testing of the temperature-sensing system in steady-state and transient-temperature conditions up to 1220°F. The following paragraphs describe the test equipment and instrumentation and the test procedures and results.

4.2 TEST EQUIPMENT AND INSTRUMENTATION

The overall bench-test system is shown in Figure 17. The setup consists of a system to heat air up to 1220°F at 1/2 lb per min airflow and a solenoid valve to perform a temperature step function from ambient temperature to 1000°F, approaching a step response of 1 msec. Figure 18 shows a sketch of the heating system, with the step-function valve and the fluidic sensor attached.

The analog computer, shown at the extreme right in Figure 17, was used to accurately establish the time response of the sensor system. Figure 19 shows the heater, output frequency counter, and readout instrumentation console. Figure 20 is a close-up view of the fluidic temperature sensor mounted in the bench-test system.

The thermocouple leads shown from the sensor and the inlet line (Figure 20) extend from high-response thermocouples used to calibrate the sensor.

An infrared detector was selected to read the output of the thermocouple because of its accuracy and speed of response. A 1/2-inch sapphire window, mounted in a "T" section immediately downstream from the slide valve, was used to transmit the infrared rays from the tube. By using a lead-sulfide infrared detector with the sapphire window, the infrared region between 0.60 and 4.50 microns was detected.

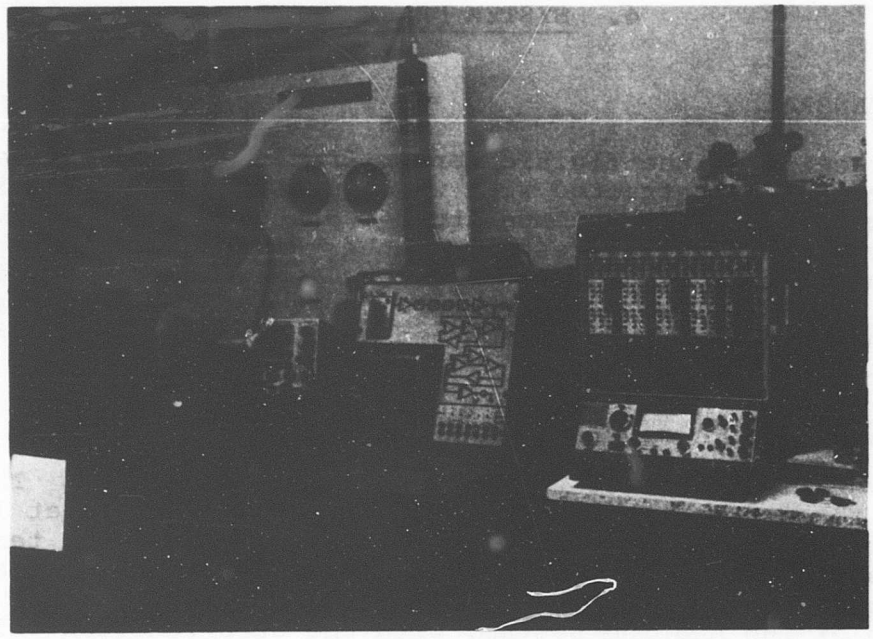

Figure 17. Bench-Test System.

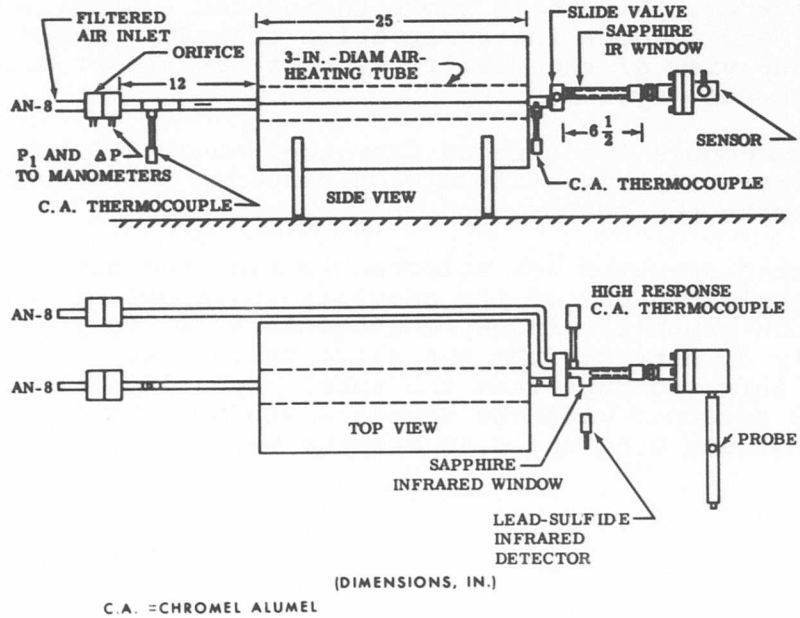

Figure 18. Temperature-Sensing System Bench-Test Diagram.

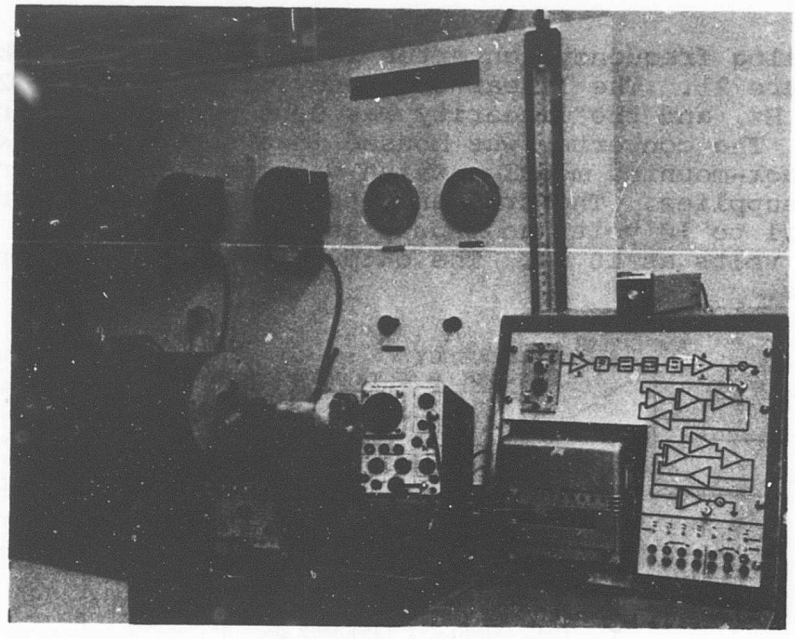

Figure 19. Heater, Output Frequency Counter, and Readout Instrumentation Console.

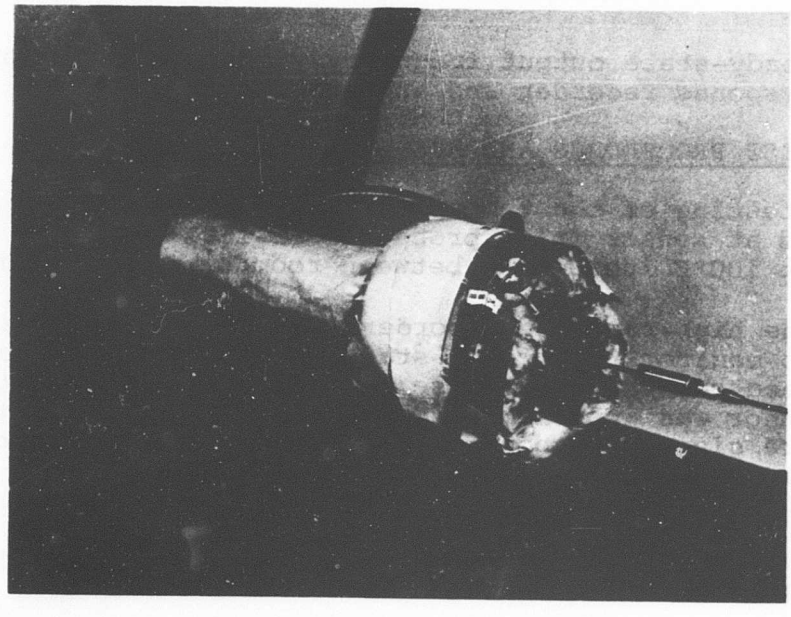

Figure 20. Fluidic Temperature Sensor Mounted in Bench-Test System.

The analog frequency converter is shown in the block diagram in Figure 21. The linear frequency range was from 2,000 to 16,000 Hz, and the linearity was 0.08 percent within this range. The converter was housed in a separate 19- x 3-1/2-inch rack-mounted module, which was complete with internal power supplies. The frequency-to-analog converter required from 0.1 to 10 volts ac input, and at 16,000 Hz the output was 10 volts at 10 ma. The output impedance was approximately 20 ohms.

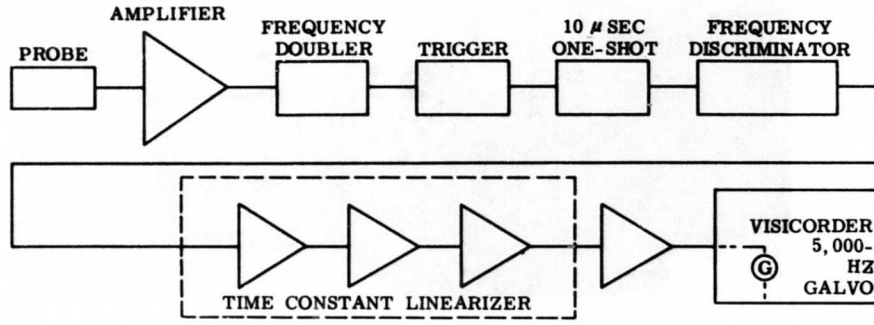

Figure 21. Block Diagram of the 2400°F Temperature Sensor Electrical Readout Circuit.

The steady-state output frequency signal was monitored by a high-response recorder and an oscilloscope.

4.3 TEST PROCEDURES AND RESULTS

Bench testing of the temperature-sensing system was accomplished at sensor inlet pressures of 150, 125, 100, and 75 psig at 100°F increments between room temperature and 1200°F.

Both the high-response recorder and the oscilloscope that were used to monitor the steady-state output-frequency signal indicated considerable noise in the output. The signal from the sensor was approximately 0.1 volt, with a peak-to-peak pressure signal of about 10 psi. The signal was recognizable as a sine wave with considerable noise.

Figures 22 through 25 show frequency-versus-temperature curves. The reference line is the frequency-versus-temperature relationship established by the vendor. The reference line was obtained by the vendor at an inlet-sensor pressure of approximately 130 psig. The table below presents the effect of pressure on the output frequency of the sensor for various steady-state temperatures. It is interesting to note that as the temperature increases, the effect of inlet pressure also increases. For a frequency of 9743 Hz at 150 psig, the actual temperature is 1125°F, which is 4.52 percent lower than predicted. This was the greatest observed pressure effect and was repeatable on the same bench setup.

With completion of the tests, the fluidic temperature-sensing system bench test setup was disassembled, and preparations were initiated for the cascade-type test evaluation.

PRESSURE EFFECT ON OUTPUT FREQUENCY OF SENSOR

Temperature (°F)	Vendor Freq. Data at 130 PSIG (Hz)	In-House Bench-Test Freq Data at Various Pressures			
		150 PSIG (hz)	125 PSIG (Hz)	100 PSIG (Hz)	75 PSIG (Hz)
0	5530	5530	5530	5530	5525
100	6032	6032	6030	6032	6000
200	6487	6525	6487	6487	6440
300	6905	6950	6910	6915	6860
400	7294	7355	7300	7304	7250
500	7657	7750	7665	7670	7630
600	8000	8100	8012	8020	7960
700	8326	8475	8350	8350	8270
800	8636	8790	8660	8655	8575
900	8930	9110	8975	8944	8880
1000	9215	9400	9245	9230	9185
1100	9480	9680	9540	9490	9400
1200	9743	9943	9800	9750	9688

NOTE: The in-house data are taken from curves selected as the best fit to the acquired bench-test data.

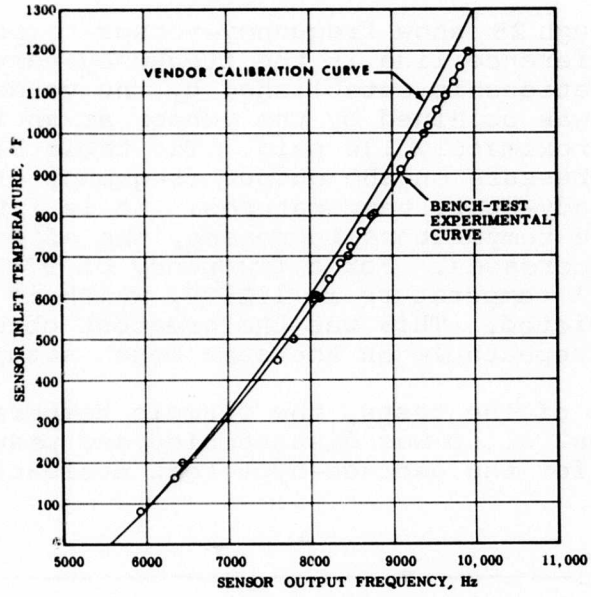

Figure 22. Bench-Test Frequency Versus Temperature for 150-PSIG Inlet Pressure.

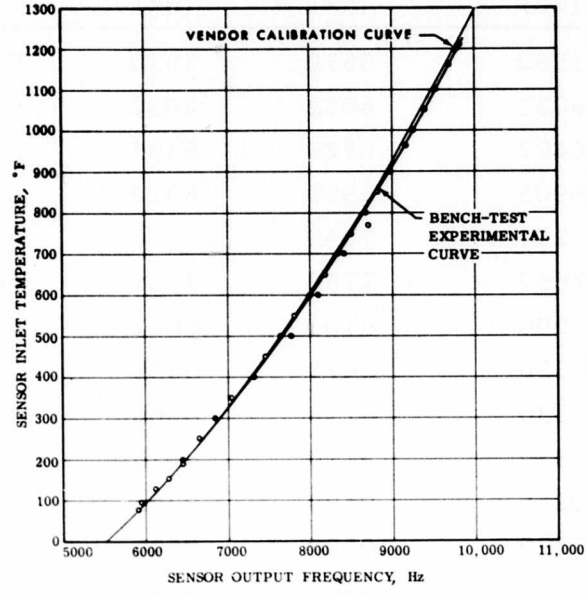

Figure 23. Bench-Test Frequency Versus Temperature for 125-PSIG Inlet Pressure

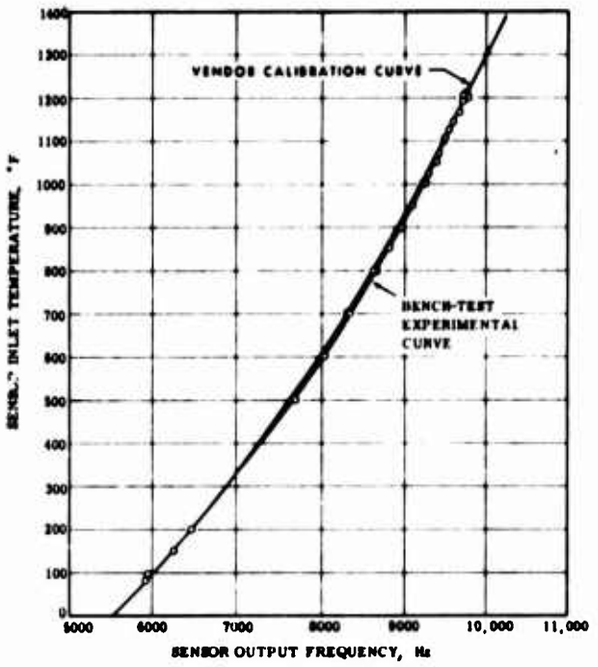

Figure 24. Bench-Test Frequency Versus Temperature for 100-PSIG Inlet Pressure.

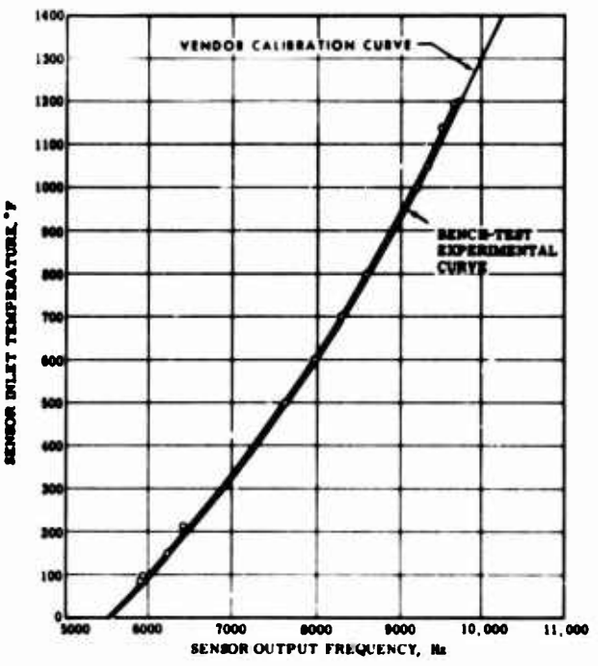

Figure 25. Bench-Test Frequency Versus Temperature for 75-PSIG Inlet Pressure.

5. SYSTEM CASCADE TESTS

5.1 GENERAL

As reported in Volume I of the uncooled-turbine final report, a high-temperature-cascade test rig was designed and developed, including instrumentation, combustors, and a control system, that simulated temperature conditions encountered during starting and normal operation of a 2400°F turbine with the design parameters of the uncooled turbine. It was this cascade test rig that was utilized for evaluation of the fluidic temperature-sensing system. The following paragraphs describe the test equipment and instrumentation that were employed and the steady-state and transient testing that was accomplished in the cascade test evaluation.

5.2 TEST EQUIPMENT AND INSTRUMENTATION

The cascade test rig and control system are described in Section 3 of Volume I. Figure 26 shows the fluidic temperature sensor installed in the cascade test rig. The cascade test-rig operator control panel is shown on the left-hand side of Figure 27. The instrumentation used during the cascade testing is shown on the right-hand side of Figure 27 and in Figure 28. The instrumentation setup that was used for the transient testing is shown schematically in Figure 29.

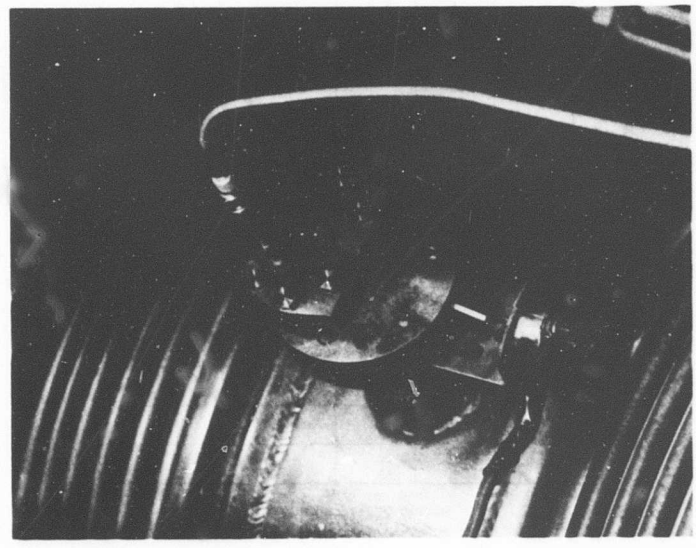

Figure 26. Fluidic Temperature Sensor Installed in Cascade Test Rig.

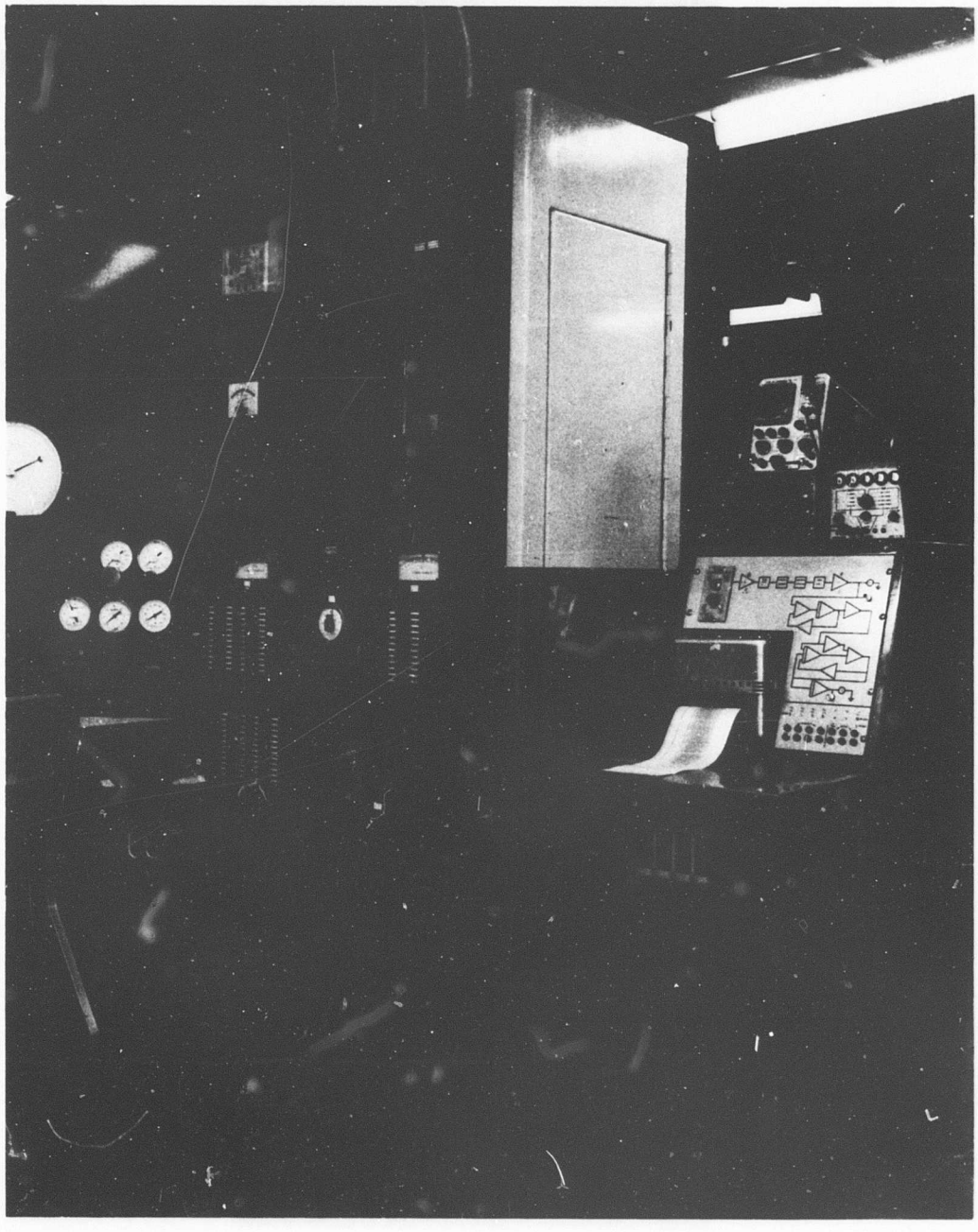

Figure 27. Cascade Test Rig Control Panel and Test Instrumentation.

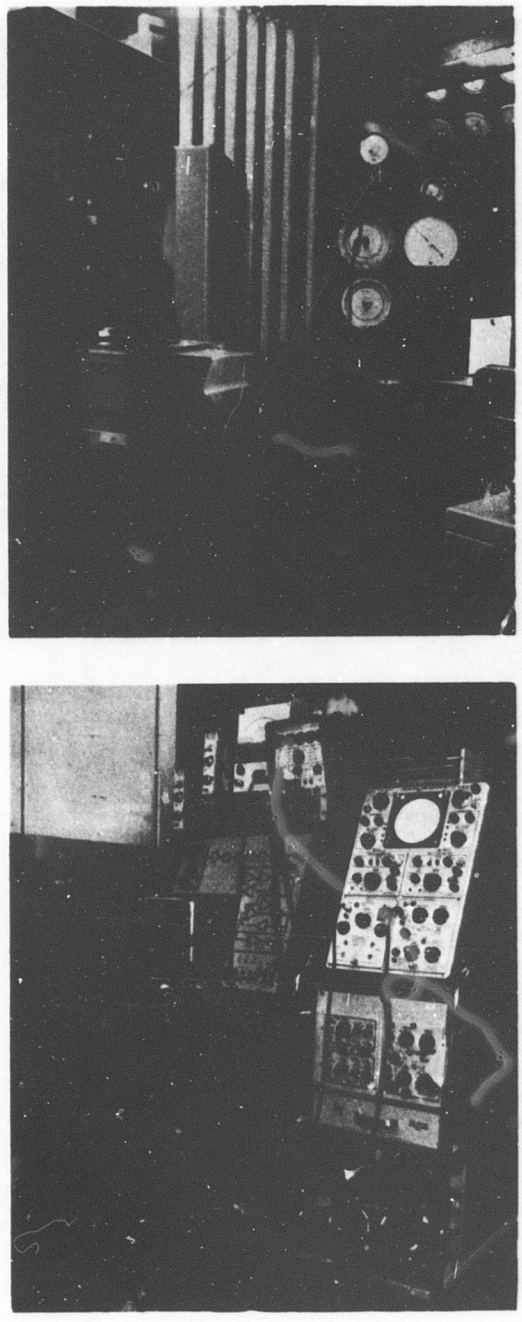

Figure 28. Two Views of Test Instrumentation Used for Cascade Testing.

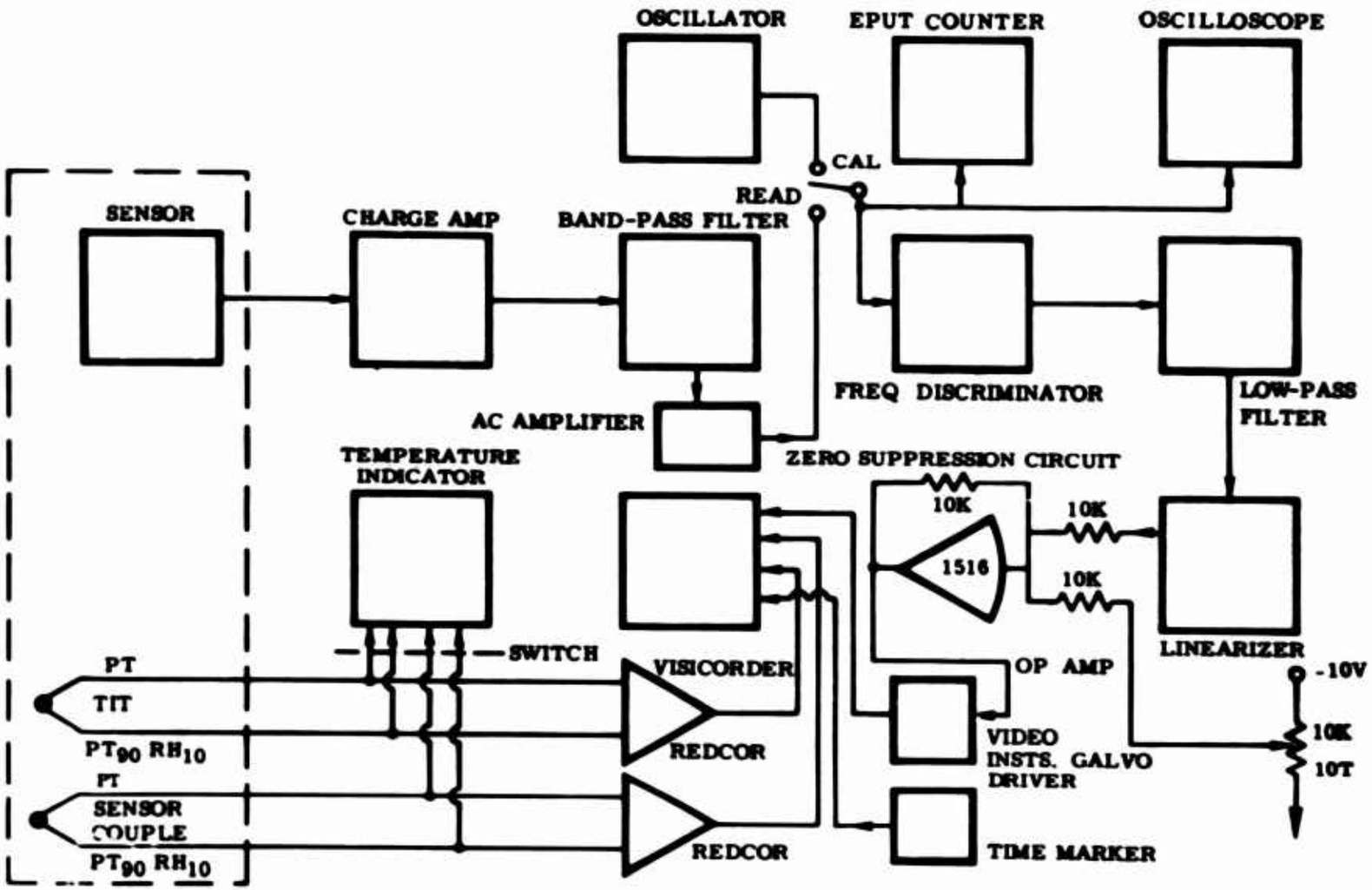

Figure 29. Schematic of Transient Test Instrumentation Setup.

5.3 STEADY-STATE TESTING

Steady-state tests were conducted in the cascade test rig at temperatures from 800° to 2400°F. The temperature was increased in increments of 100°F, and the sensor inlet pressure was maintained at 146 psig.

Figure 30 shows the frequency-versus-temperature relationship obtained by the vendor (at 130-psig sensor inlet pressure). The in-house test data deviated a maximum of 1.2 percent (lower frequency output) from the vendor's data. This deviation was in the expected tolerance band.

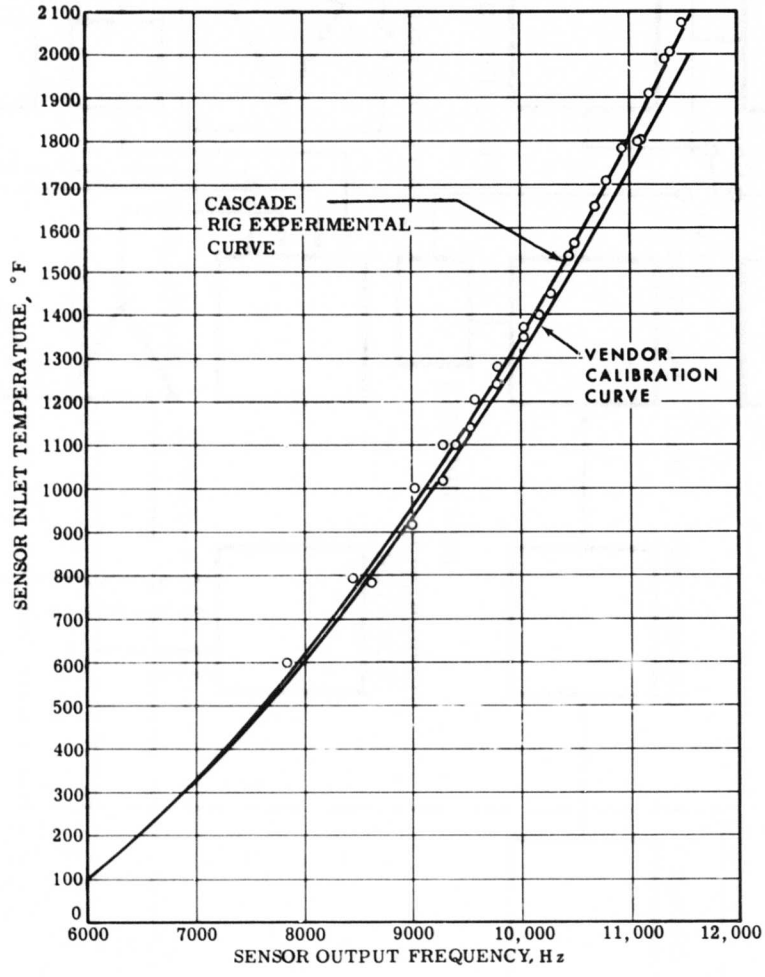

Figure 30. Steady-State Test Data for 146-PSIG Sensor Inlet Pressure.

5.4 TRANSIENT TESTING

The transient tests that were conducted in the cascade test rig were accomplished in two phases, with an interval period during which bench-test correlations, system rework, and steady-state testing were accomplished.

The problem of measuring the sensor dynamic response differs from that of determining the sensor frequency-versus-temperature relationship of the steady-state testing because of the electronic equipment required to interpret the transducer signal. If the signal is a pure sine wave, the dc output of the converter will indicate a steady-state level proportional to the frequency. If the input signal has a noise or a modulated signal, the converter will respond to the small variations in frequency change due to the noise. This susceptibility to noise must be present for the converter to respond to step changes in temperature. The dc output to the converter will have a mean-average level proportional to the predominant input frequency, but it will vary about the mean level due to small frequency changes (noise).

Most digital counters sample input frequencies for 1 second and, therefore, do not display the noise changes except as a last digit change over several readings. The counter will always display a smaller perturbation about the mean, since its response is considerably less than the frequency-to-analog converter. Any filtering of the input or output signals of the converter will reduce the response of the output signal.

5.4.1 Phase I Testing

Transient test runs were accomplished in the high-temperature-cascade testing of Phase I. Four classes were conducted:

1.	700° to 2600°F	2 sec
	2600° to 2000°F	3 sec
2.	700° to 2400°F	4 sec
	2400°F steady-state	300 sec
3.	700° to 2400°F	10 sec
	2400°F steady-state	300 sec

4.	700° to 1600°F	2 sec
	1600° to 700°F	4 sec
	700° to 2000°F	2 sec
	2000° to 700°F	4 sec
	700° to 2400°F	2 sec
	2400° to 700°F	4 sec
	700° to 2600°F	2 sec
	2600° to 700°F	4 sec

The runs were to be initially recorded without corrections of the output signal in order to determine the required thermal inertia correction. The signal would then be corrected with the use of a correction circuit to provide a temperature-measurement system with a maximum overall time constant of 10 msec.

The output signal of the sensor was too noisy to provide a record with which to work. This problem could not be satisfactorily solved. The various investigations performed to eliminate this problem are described below. The transducer of the sensor was found to be transmitting a noisy signal; therefore, the sensor was removed from the cascade rig and disassembled for inspection. Six of the seven bolts of the sensor were found to have failed during the 9 hours of operation in the cascade test rig. Little evidence was found to indicate either erosion or clogging of the sensor cavity and sensor ports. Figure 31 shows the condition of the bolts as they were taken from the sensor.

The sensor was refurbished with new bolts made of Inconel 702, and a new transducer was installed.

Cold tests were initially performed to determine the effect, if any, of the new bolts and transducers on the output of the sensor. No deviation from previous cold-test results was noticeable. The sensor was installed again in the high-temperature-cascade rig. The signal received by the recorder and the oscilloscope was again too noisy to permit the dynamic response to be measured. This noise was found to be generated by the sensor transducer and not the instrumentation equipment. The noise level was excessive over the entire temperature range. The sensor inlet pressure was varied from 75 psig to a maximum value of 156 psig at 100°F temperature increments up to 2400°F without noticeable effect on the excessive noise level.

There was some question as to whether or not the cascade test rig was subjecting the sensor and sensor pressure transducer to excessive vibration. If this were the case, the noise found in the sensor signal might very well be caused by the cascade test rig and not by the sensor. To check this possibility, it was decided to remove the sensor from the cascade test rig and check the noise level in the bench test rig.

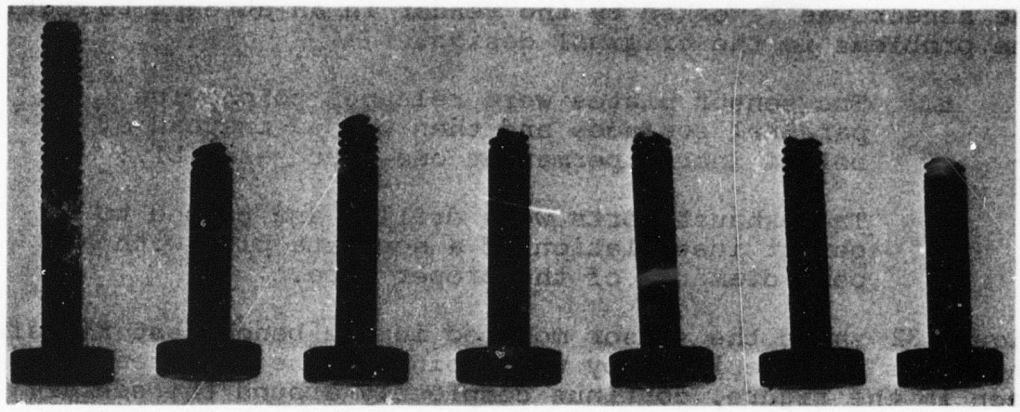

Figure 31. Bolts Holding Fluidic Temperature Sensor Together After 9 Hours in the 2400°F Turbine Research Cascade Test Rig.

5.4.2 Interim Bench Testing, System Rework, and Steady-State Testing

The sensor was installed in the bench-test rig, and the noise level of the sensor signal was determined to be essentially the same as that experienced in the cascade test rig.

Next, the sensor was checked in the bench-test rig without the probe to determine if the gas transfer probe, which is bolted directly to the sensor, might be causing the transducer noise. No appreciable difference in sensor output wave form was detected. For this bench test, the sensor was checked cold (75°F) at various pressure levels without the probe in place.

The sensor was then returned to the vendor for inspection and possible rework necessary to eliminate the sensor signal noise. The following is a summary of the vendor's findings:

1. The top and bottom plates were warped, which permitted excessive leakage. (The vendor considered this to be a prime source of the signal noise.)

2. The exhaust ports were eroded to an extent that prevented proper signal generation.

3. The bolts (second set) holding the sensor together were broken due to differential thermal expansion.

The sensor was reworked by the vendor in an attenpt to rectify the problems in the original design.

1. The sensor plates were relapped to provide parallel surfaces and then welded instead of bolted into a permanent one-piece assembly.

2. The exhaust ports were drilled and tapped to permit installation of a separate plug with a port diameter of the proper size.

Figure 32 shows the sensor mounted in the bench test rig after the bolts were replaced by weld joints. The weld seams, as seen in the figure, continue completely around the sensor. This approach was taken to eliminate leakage between the plates and to remove the tensile load from the bolts, preventing repeatable inspection of the sensor cavity. However, this loss of inspection capability was considered to be a reasonable trade-off for a working sensor.

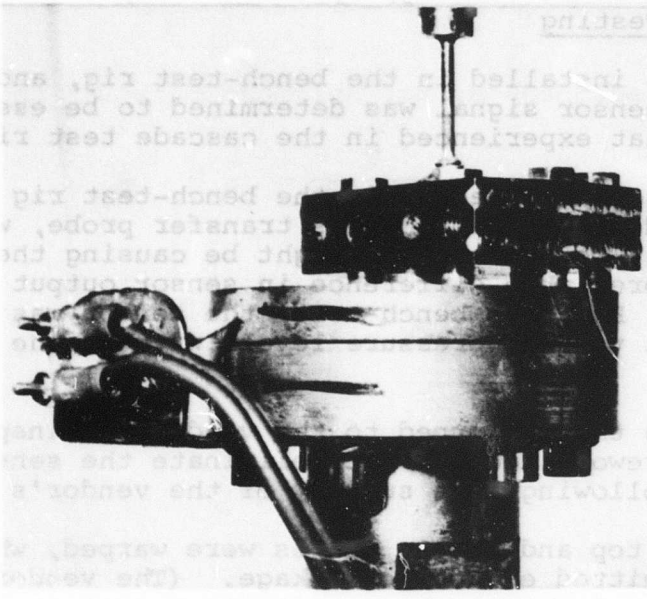

Figure 32. Mounted Sensor as Received After Vendor Modifications.

The vendor suggested that the sensor be bench-tested with exhaust-port plugs of different exhaust areas, as shown by Figure 33. Tests on the sensor output signal obtained from output ports with 0.030-, 0.028-, and 0.020-inch diameters showed no improvement in sensor output signal when using the smaller exhaust ports.

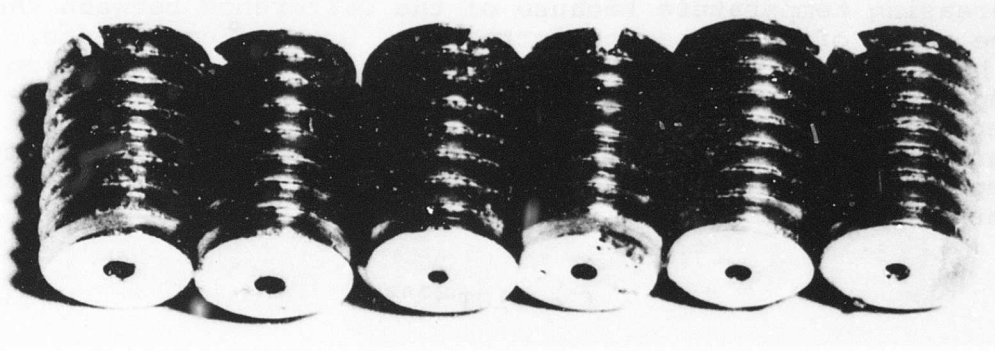

Figure 33. Exhaust-Port Plugs (Three Sets).

Because of the results of these tests, the ports were completely removed from the sensor to determine the effect on the output. The performance of the sensor at temperatures of 70°F, 700°F, 950°F, and 1120°F, with no exhaust-port plugs, was improved. Upon completion of the test, a detailed inspection of the sensor revealed that the holes that had been drilled and threaded to accommodate the removable exhaust port plugs had not been drilled completely through the sensor body wall. Consequently, the original integral exhaust orifices were still effective when the sensor was tested with the removable exhaust port plugs removed.

With the bench test showing a good output signal, with the integral orifices employed, it was decided to continue the sensor evaluation in the 2400°F cascade test rig.

Steady-state testing was accomplished to determine the static frequency-versus-temperature relationship of the sensor by slowly increasing and decreasing the temperature (as determined by the sensor inlet thermocouple) and recording frequency and temperature data at 100°F intervals from 400° to 2000°F. This was done at a sensor inlet pressure of 145 psig.

Figure 34 shows the results of the static calibration tests of the sensor and the data points determined from a bench-check static calibration performed in the bench-rig test setup. These data points agree well with those determined in the cascade rig for slowly increasing temperature. The data for decreasing temperature differ from those for increasing temperature because of the difference between the time rates of decrease and increase of sensor temperature. It has been observed that the sensor must remain at a given temperature for a long time in order to obtain a valid frequency reading. This characteristic is unfavorable for transient-temperature-measuring applications. The frequency-temperature function derived from the increasing temperature static calibration was

$$f = 710T^{0.352} \tag{30}$$

where T = temperature, °R

f = frequency, Hz

5.4.3 Phase II Testing

Transient tests were performed to evaluate the sensor linearized response to rapid changes in sensor inlet temperature. For this purpose, a high-response (10 msec) thermocouple was installed in the sensor inlet, and the output of this thermocouple was compared to the sensor linearized output signal. Both signals were compared to the main gas temperature at the sensor insulating hood connecting-tube inlet by the use of an aspirated thermocouple located near the connecting-tube inlet.

It was necessary to include a band-pass filter and amplifier in the instrumentation to obtain a usable frequency signal from the sensor. A zero suppression circuit was used to obtain a greater span of the Visicorder for the sensor linearized signal. The linearizer calibration was adjusted to correspond to Equation (30). The sensor linearized signal was attenuated with a video instrumentation galvo driver to obtain 400°F per inch deflection on the Visicorder. The sensor thermocouple and TIT thermocouple were connected to amplifiers. The output of each amplifier was connected to the Visicorder. The gains of the amplifiers were adjusted to obtain 400°F per inch deflection on the Visicorder. Calibration data for $Pt_{.90}Rh_{.10}$-Pt thermocouples in the 700° to

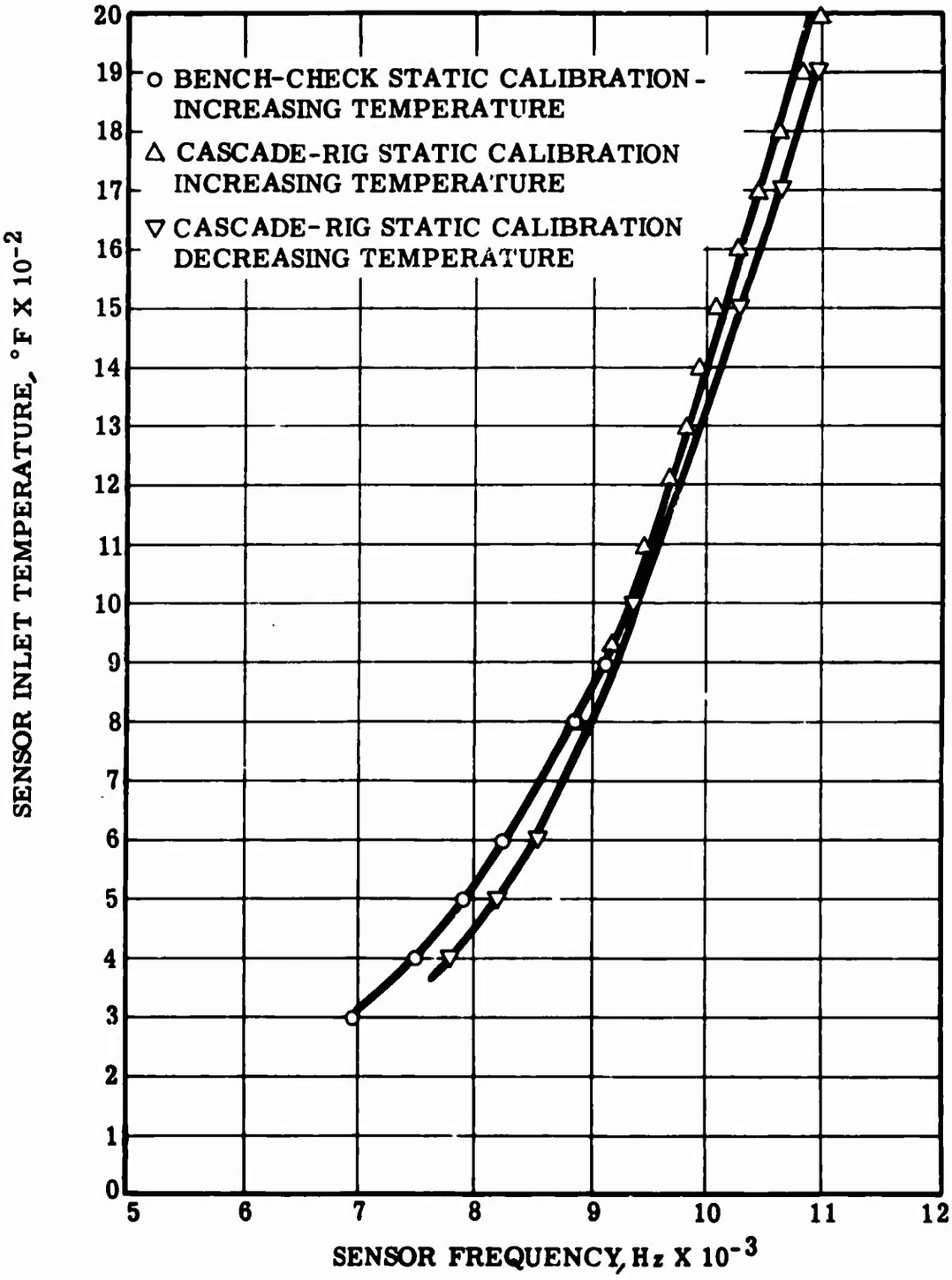

Figure 34. Bench-Check and Combustion-Rig Static Calibrations of Fluidic Temperature Sensor.

2200°F range were used in adjusting the amplifier gains. Base-level temperatures were read out on an indicator. Sensor inlet pressure was maintained at 145 psig at the lower temperatures and at 135 psig at the higher temperatures.

Figure 35 shows the transient response of the sensor, sensor inlet thermocouple, and TIT thermocouple for one transient temperature. The true TIT cannot be determined exactly, since the precise time-constant of the TIT thermocouple is not known. Analytically, an approximation to the true TIT can be made based upon the observed response of the TIT thermocouple. The transfer function of the TIT thermocouple was approximately

$$H(s) = \frac{1}{s\tau_1 + 1} \tag{31}$$

where τ_1, the time-constant of the TIT thermocouple, is approximately 0.2 second.

The observed response from the TIT thermocouple may be approximated by

$$G(t) = T_0 \left[1 - e^{-t/\tau_2}\right] \tag{32}$$

Therefore, the transfer function can be described as

$$G(s) = \frac{T_0}{s(s\tau_2 + 1)} \tag{33}$$

The Laplace transform of the actual input temperature is found from the definition of the transfer function. Since all initial conditions were zero in determining G(t), we have

$$H(s) = \frac{G(s)}{F(s)} \tag{34}$$

where F(s) is the Laplace transform of actual input temperature. Thus,

$$F(s) = \frac{G(s)}{H(s)} = \frac{T_0(s\tau_1 + 1)}{s(s\tau_2 + 1)} \tag{35}$$

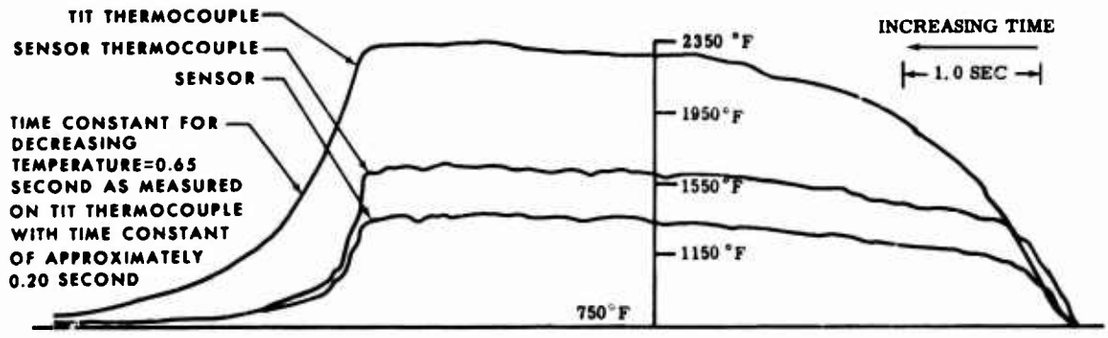

Figure 35. Transient Response of Sensor, Sensor Thermocouple, and TIT Thermocouple.

Using the inversion integral to get F(t) gives

$$F(t) = T_o \left[1 - \frac{(\tau_2 - \tau_1)}{\tau_2} e^{-t/\tau_2} \right] \tag{36}$$

Thus, if $\tau_1 = \tau_2$, the input temperature F(t) would be a step function.

From Figure 35, the value of τ_2 is approximately 0.65 second. Assuming that τ_1 is 0.20 second, then

$$F(t) = T_o \left[1 - 0.7e^{-t/\tau_2} \right] \tag{37}$$

Equation (37) is sketched below.

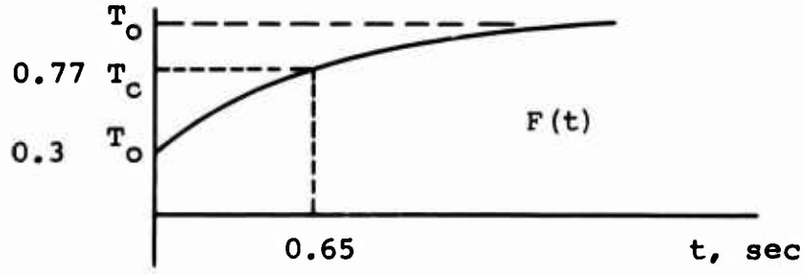

Figure 35 shows that, under transient conditions, the maximum temperature reached by the TIT thermocouple was about 1.7 times that reached by the sensor-inlet thermocouple. Also, the maximum temperature indicated by the sensor-inlet thermocouple was about 1.4 times that indicated by the sensor linearized output. The sensor-inlet thermocouple and the sensor showed very nearly the same form of response. That form of the response corresponds closely with Equation (36).

The fact that the sensor linearized output did not indicate the same amplitude as the sensor inlet thermocouple supported the conclusion, derived from the static calibration that the sensor required a long time to achieve the correct frequency for a given temperature level.

The curve-correction circuits designed for the sensor evaluation were not used in this series of transients, in order to determine the transient response of the sensor without benefit of the circuits.

Upon completion of the Phase II transient testing, the sensor, sensor splitter, and probe were examined to determine if the prolonged exposure (in excess of 100 hours) to temperatures in the 2400°F range had any effect on the material. Examination of the components revealed no material discrepancies or defects as a result of the temperature exposure.

6. CONCLUSIONS

The objective of the fluidic temperature sensor program--to determine the feasibility of a fluidic temperature sensing system for TIT measurement in a 2400°F turbine--was accomplished. However, the conclusion reached was that the system, as tested, was not a feasible means of TIT measurement. Conditions leading to this conclusion are discussed below.

6.1 RESPONSE TO TEMPERATURE TRANSIENTS

The long time-constants that were demonstrated by the fluidic temperature sensing system substantiated that this system, as tested, would not be adequate for applications that require high response to temperature transients.

6.2 ACCURACY VARIATIONS

It was revealed during the test program that the sensor inlet pressure had a much greater effect on the accuracy of the fluidic sensor output frequency than had been anticipated. It had been expected that a pressure level would be found, above which changes in pressure would have no effect on sensor performance. No such pressure level was found.

It was found that as the temperature was increased, the effect of sensor inlet pressure on the sensor performance also increased. The worst condition was found at 150 psig inlet pressure and 1125°F, where the error in the temperature readout was approximately 4-1/2 percent. This error is too large, by at least a factor of 4, for the sensor system to be a useful device for measuring TIT.

6.3 RELIABILITY OF SENSOR

The sensor fabricated from three plates held together by through-bolts was found to be unsatisfactory because of excessive leakage and bolt failures. It is expected that the sensor will require one-piece fabrication to provide satisfactory operation over a long period of time. An investment casting would be an attractive approach for the fabrication of such a sensor.

6.4 OPERATION AND READOUT

The greatest limitation of the fluidic temperature sensing system is the readout system. The system as evaluated would

not be practical, for two basic reasons: it is too expensive and it is too cumbersome. A temperature-measuring system must be relatively inexpensive (comparable to an equally efficient thermocouple system) and simple in operation. The sensor body is a very cheap and simple part to fabricate; the expense and sophistication lie in the method of converting the sensor signal into a usable form. Until a simple and direct approach is conceived, the sensor will probably not find its way into small gas turbine applications.

7. RECOMMENDATIONS

Although the practicability of a fluidic temperature-sensing system for TIT measurements in the 2400°F range with transient rates reaching 2500°F per second was not demonstrated by this program, it is recommended that further research be conducted to resolve the established limitations. Demands for increasingly higher turbine operating temperatures have created the need for more precise control of an engine during transient conditions and while operating at the increased temperature levels. Such engine control can be accomplished only if a much more accurate and responsive method of measuring TIT is developed than is presently available.

It is believed that the possible advantages and limitations of a fluidic temperature-sensing system revealed by this program indicate that such a system affords enough potential to warrant continued research. Recommendations are listed below for improvement of the tested system.

1. Improvement of the transient-temperature response characteristics of the sensor could be accomplished by design changes to:

   (a) Mount the sensor in such a way that intimate contact with the gas stream is always maintained.

   (b) Provide the smallest sensor-body mass thermal inertia possible by reducing the sensor-body volume and the sensor-body wall thickness as much as is technically feasible.

2. Research efforts should be directed toward reducing the adverse effect on readout accuracy produced by variations of the inlet pressure.

3. Reliability of the sensor could be improved by utilization of fabrication methods that would produce a one-piece sensor.

4. Research efforts should be directed toward development of a readout system that is both effective and inexpensive to produce. A program that could optimize this particular area of technology would provide the greatest single achievement necessary for the successful use of a fluidic temperature-sensing system.

Unclassified

Security Classification

DOCUMENT CONTROL DATA - R & D

(Security classification of title, body of abstract and indexing annotation must be entered when the overall report is classified)

1. ORIGINATING ACTIVITY (Corporate author)
AiResearch Manufacturing Company
402 S. 36th Street
Phoenix, Arizona

2a. REPORT SECURITY CLASSIFICATION
Unclassified

2b. GROUP

3. REPORT TITLE
2400°F UNCOOLED TURBINE/MATERIAL PROGRAM
VOLUME III - FLUIDIC TEMPERATURE-SENSING SYSTEM EVALUATION

4. DESCRIPTIVE NOTES (Type of report and inclusive dates)
Final Technical Report

5. AUTHOR(S) (First name, middle initial, last name)
Paul R. Craig
Fritz Weber

6. REPORT DATE
July 1970

7a. TOTAL NO. OF PAGES
64

7b. NO. OF REFS

8a. CONTRACT OR GRANT NO.
DA 44-177-AMC-183(T)

b. PROJECT NO.
Task 1G162203D14413

c.

d.

9a. ORIGINATOR'S REPORT NUMBER(S)
USAAVLABS Technical Report 70-32C

9b. OTHER REPORT NO(S) (Any other numbers that may be assigned this report)

10. DISTRIBUTION STATEMENT
This document is subject to special export controls, and each transmittal to foreign governments or foreign nationals may be made only with prior approval of U. S. Army Aviation Materiel Laboratories, Fort Eustis, Virginia 23604.

11. SUPPLEMENTARY NOTES
Volume III of a 3-volume report

12. SPONSORING MILITARY ACTIVITY
U. S. Army Aviation Materiel Laboratories
Fort Eustis, Virginia

13. ABSTRACT

A fluidic temperature sensor was designed and evaluated in a 2400°F cascade test rig to establish its feasibility as a turbine inlet temperature sensing device. The cascade test rig was designed and developed as part of a program to advance the technology of a small 2400°F uncooled turbine component (Volumes I and II). The fluidic sensor evaluation included procurement and analytical evaluation of a fluidic sensor design, selection of materials for a breadboard-type sensor to fit the requirements of the 2400°F cascade test rig, checkout and calibration of the sensor on a bench test rig, and transient and steady-state testing of the sensor in the 2400°F cascade test rig.

It was concluded that without additional research and development efforts, it is not feasible to use the tested fluidic temperature sensor in a 2400°F turbine.

DD FORM 1 NOV 68 1473 REPLACES DD FORM 1473, 1 JAN 64, WHICH IS OBSOLETE FOR ARMY USE.

Unclassified

Security Classification

14. KEY WORDS	LINK A		LINK B		LINK C	
	ROLE	WT	ROLE	WT	ROLE	WT
Fluidic Temperature Sensor						
2400°F Uncooled Turbine						
Turbine Inlet Temperature Measurement						